10 The Witwatersrand Basin and Its Gold Deposits

Hartwig E. Frimmel

Abstract

The Mesoarchaean Witwatersrand Basin represents the largest known gold anomaly and has produced more gold than any other ore province in the world. Deposition of the predominantly siliciclastic basin fill began shortly after 2985 Ma in a shallow marine environment, maybe along a passive margin to an old continent to the north (west), and under generally cool climatic conditions (West Rand Group). Tectonic inversion following the extrusion of 2914 Ma andesitic lava led to a shift towards continental sedimentation. Following a basin-wide hiatus at around 2900 Ma, the largely arenitic Central Rand Group was deposited into a retroarc foreland basin that regressed as it was filled between <2902 and >2780 Ma in response to crustal accretion along the western and northern margins of the basin. This stage was accompanied by the largest known concentration of gold in Earth's history, initially by microbial fixation on emerging colonies of probably cyanobacteria in near-coastal environments, subsequently by mechanical reworking of the gold-rich microbial mats to form conglomerate-hosted placer deposits. The source of the huge amount of gold in the Witwatersrand is thought to be the entire greenstone-dominated Archaean cratonic surface, which was subjected to intensive chemical weathering permitting large-scale leaching of gold by contemporaneous surface waters. Syn-depositional tectonism that extended from the hinterland into the foreland basin led to repeated further physical reworking of gold-rich sediments to form more placer deposits higher up in the stratigraphy, even above the Witwatersrand Supergroup. The Witwatersrand Basin fill was subjected to a series of alteration events, ranging from burial and regional low-grade metamorphism to heating in the course of the emplacement of the 2054 Ma Bushveld Igneous Complex and catastrophic shattering during the 2023 Ma Vredefort impact, which enabled renewed fluid flow long after primary rock porosity had been obliterated. This caused some short-range mobilisation of ore components, including gold, but without changing the overall sedimentological and stratigraphic control on ore grade.

Keywords

Witwatersrand • Gold • Mesoarchaean • Kaapvaal Craton

10.1 Introduction

The Witwatersrand Basin near the centre of the Kaapvaal Craton (Fig. 10.1) is a domain of many superlatives and holds several world records. Foremost it has become famous for representing the by far largest known gold anomaly in the world. The Witwatersrand goldfields (Fig. 10.2) have produced, with some 53,000 t Au, about one-third of all the gold that has ever been mined in history, and estimated remaining resources account for close to 30% of global known resources (Frimmel 2014), though much of this is beyond the reach of conventional and currently economic mining methods. For many decades, they were the world's leading producer of gold, although the more easily accessible ores have largely been exploited, and annual production has followed a steady downwards trend since 1970. Apart from the exceptional endowment in gold, the Witwatersrand ores also represent one of the world's major uranium resources. Within some of the gold-bearing conglomerates, a total resource of >200 kt U_3O_8 is still present, but most of the uranium, where it has not been extracted, is now

H. E. Frimmel (✉)
Department of Geodynamics and Geomaterials Research, Bavarian Georesources Centre, Institute of Geography and Geology, University of Würzburg, Am Hubland, 97074 Würzburg, Germany
e-mail: hartwig.frimmel@uni-wuerzburg.de

H. E. Frimmel
Department of Geological Sciences, University of Cape Town, Rondebosch, 7701, South Africa

A. Kröner and A. Hofmann (eds.), *The Archaean Geology of the Kaapvaal Craton, Southern Africa*, Regional Geology Reviews, https://doi.org/10.1007/978-3-319-78652-0_10

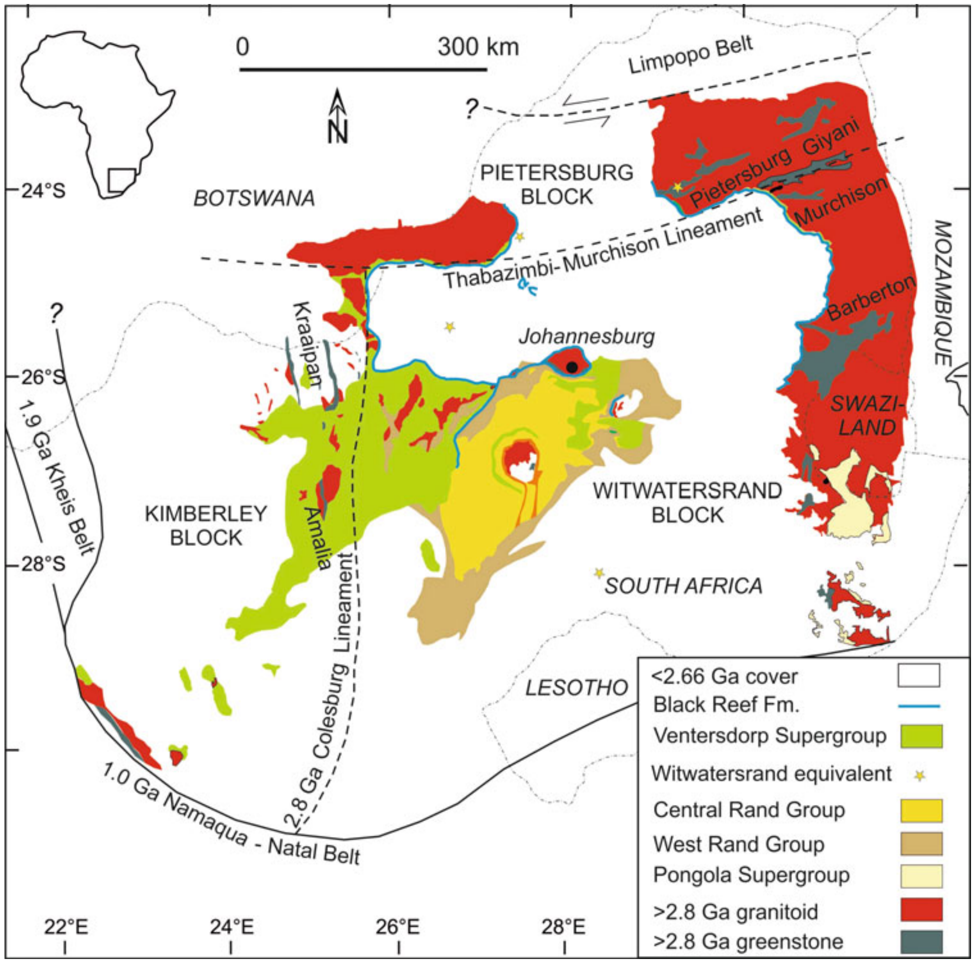

Fig. 10.1 Surface and sub-surface distribution of the main Archaean stratigraphic units of the Kaapvaal Craton, showing the known extent of the Witwatersrand Basin, the fill of which comprises the West Rand and Central Rand groups; blue line delineates trace of the Black Reef Quartzite Formation at the base of the Neoarchaean to early Palaeoproterozoic Transvaal Basin; from Frimmel and Hennigh (2015); stars indicate positions of Witwatersrand-equivalent rocks having been intersected in drill core

concentrated in voluminous tailings dams, totalling close to 1 Mt U_3O_8. This huge amount of uranium constitutes, with close to 10%, the world's third largest uranium resource in terms of deposit type (Frimmel 2010) and poses one of the largest mining-induced environmental health risks.

Thanks to more than a century of mining and exploration, there is hardly any other area in the world whose underground geology has been three-dimensionally documented to the same extent as in the Witwatersrand. From a technical point of view, some of the leading tools in the exploration industry have been developed there. As early as 1889 diamond drilling led to the discovery of sub-surface extensions of gold-bearing conglomerates. The discovery of the Carletonville and Welkom goldfields in the 1930s and in 1946, respectively, was based on the pioneering use of magnetometer and gravimeter. With close to 4 km below surface, today some of the mines in the Witwatersrand are the deepest in the world.

Although rocks of the Witwatersrand Supergroup are hardly exposed on surface, they can be regarded as the best-preserved and most intensely investigated Mesoarchaean sediment succession thanks to not only the intensity of mining and exploration but also a unique geological history that prevented total erosion or tectonic recycling of these ancient deposits. Thus the Witwatersrand Basin fill has become the best available record of Mesoarchaean environmental conditions and serves as a reference for the reconstruction of ancient secular changes in the composition of the atmosphere, hydrosphere and biosphere.

Last but not least, the Witwatersrand Basin hosts in its centre the world's largest and oldest known impact structure, now evident in the form of the 2023 ± 2 Ma (Kamo et al. 1996) Vredefort Dome (Fig. 10.3). Although the exceptional metal endowment of the Witwatersrand strata cannot be related to this impact because it predates this catastrophic event by some 800–900 million years, the impact had some major consequences for the auriferous sediments. The resulting impact melt sheet probably helped in preserving the underlying, much older sediments from subsequent erosion. The impact shattered the surrounding crustal rocks, especially those of the Witwatersrand Basin, whose areal extent corresponds closely to the diameter of the original astrobleme, estimated to have been some 300 km (Therriault et al. 1997). This enabled the widespread percolation of fluids and

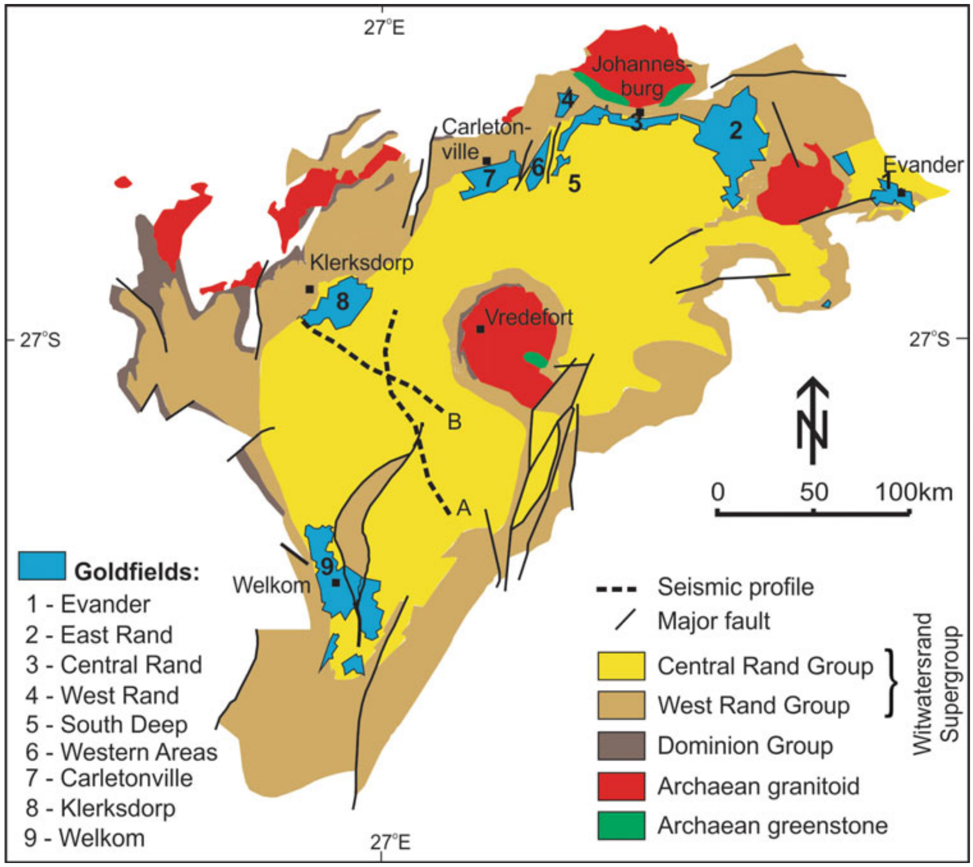

Fig. 10.2 Simplified surface and sub-surface geological map of the Witwatersrand Basin, also showing the distribution of Archaean granitoid domes, the location of the goldfields, major faults, and position of seismic profiles shown in Fig. 10.6; from Frimmel and Minter (2002)

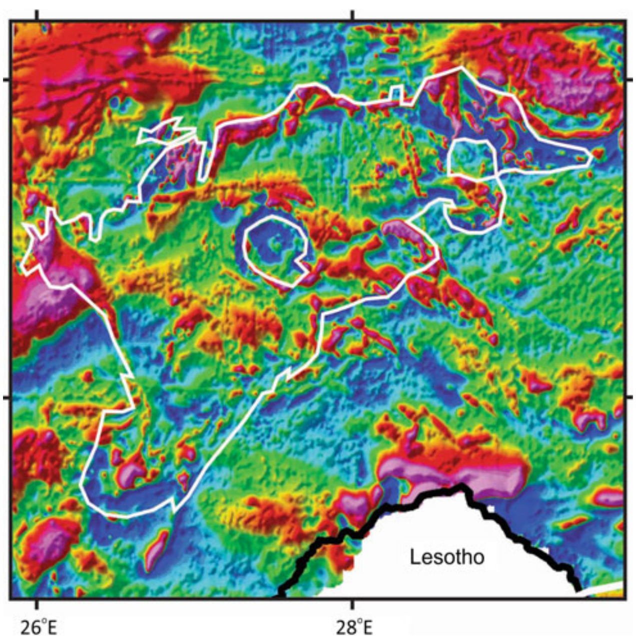

Fig. 10.3 Aeromagnetic map of the Witwatersrand Basin (extracted from map constructed by H. Jelsma based on data provided by Anglo American Corp. Ltd. for the Kaapvaal Craton Project—see South African Journal of Geology, vol. 107, p. 2, 2004); high magnetic signatures reflect ferruginous (magnetic) shales in the West Rand Group. Note the circular magnetic structure defined by the Vredefort Dome in the centre

partial remobilisation of ore components, including gold, which, in turn, led to textural and geochemical features that confused many of those who have attempted to establish the genesis of this gold province.

Almost every imaginable genetic model has been proposed to explain the Witwatersrand gold deposits, ranging from syn-sedimentary placer to epigenetic magmatic or metamorphic origins. More than 50 years ago the question of the Witwatersrand gold genesis was coined ‘the most debated issue in economic geology’ (Davidson 1965), and looking at the huge amount of literature on this topic since then, it appears as if little has changed. In spite of well over 1000 publications on the geology of the Witwatersrand, a number of fundamental questions remain unanswered. Nevertheless, tremendous advances could be made in our understanding of the geological evolution of the Witwatersrand strata, and more recently especially on their bearing on our knowledge of the evolution of the atmosphere and biosphere, both of which can be directly linked to the formation of the gold deposits.

For obvious economic reasons the focus has been on the Witwatersrand Basin as known from surface and sub-surface observations, stretching for about 350 km in a northeasterly and about 200 km in a northwesterly direction (Fig. 10.1). Stratigraphically equivalent units have been recognised also in other areas of the Kaapvaal Craton, suggesting that originally at least parts of the Witwatersrand Supergroup covered a much larger part of the craton. The largest of these equivalent units are the Mozaan Group of the Pongola Supergroup in the southeastern part of the craton, smaller ones are the Uitkyk Formation, comprising quartzites and auriferous conglomerates in the Pietersburg Greenstone Belt (de Wit et al. 1993) and others to the north and southeast of the basin (McCarthy 2006) (Fig. 10.1).

In this contribution, I summarise our current thinking on the sedimentological and tectonic history of the 'Witwatersrand Basin' which, as will be shown, was not a single coherent basin but, in fact, represents a successor basin in which the fills of different types of basins became stacked on top of each other. This will be complemented by a discussion of the changes in environmental conditions from ca. 3.0 to 2.6 Ga and their consequences on the formation of the uniquely rich gold deposits. It is impossible to give proper credit to every single worker who has contributed towards advancing our knowledge of the Witwatersrand Basin—the number of publications and theses on this topic is too vast. Review papers in which the interested reader can find a wealth of further references were published repeatedly, the more recent ones being by Robb and Meyer (1995), Robb and Robb (1998), Phillips and Law (2000), Frimmel et al. (2005), Hayward et al. (2005), McCarthy (2006), Frimmel (2014) and Tucker et al. (2016).

10.2 Litho- and Chronostratigraphy

The stratigraphic sub-division of the Witwatersrand Basin fill, in its essential parts, goes back to Mellor (1917) whose broad division into 'Lower Witwatersrand System' with the 'Hospital Hill, Government Reef' and 'Jeppestown Series', and 'Upper Witwatersrand System' with the 'Main-Bird Series' and the 'Kimberley-Elsburg Series' has withstood the test of time, albeit with slightly modified names of units and stratigraphic ranks. Mellor's two systems were renamed by SACS (1980) to West Rand Group and Central Rand Group, respectively, and his various series are now ranked as subgroups (see Fig. 10.4). The latter have been further sub-divided into formations based on basin-wide disconformities. Stratigraphic correlation between the various goldfields at the subgroup level poses no problem but is highly problematic at formation level. McCarthy (2006) provided an attempt of a unified lithostratigraphic scheme for the Witwatersrand Supergroup, and this is adopted here (Fig. 10.4).

The pre-Witwatersrand basement comprises Palaeo- to Mesoarchaean granitoid-greenstone terranes (Fig. 10.1) that are described in greater detail elsewhere in this book. The most prominent and intensely studied amongst them is the Barberton Greenstone Belt, which is well exposed farther east of today's extent of the Witwatersrand Basin fill. Its maximum and minimum ages are constrained by the 3660 ± 4 Ma Ancient Gneiss Complex in the southern part of the belt and the 3106 ± 3 Ma Nelspruit Batholith that is intrusive into the 3226 to 3209 Ma foreland deposits of the Moodies Group (Heubeck 2019). Others are the Murchison, Pietersburg and Giyani greenstone belts towards the northeast and the Amalia and Kraaipan greenstone belts to the west of the basin. Remnants of the immediate basement of the Witwatersrand Basin are today exposed, thanks to 2023 ± 2 Ma (Kamo et al. 1996) impact-induced up-doming, as a variety of high-grade metamorphic ca. 3.1 Ga gneisses and migmatites and a low-grade metamorphic mafic to ultramafic volcanic unit within the Vredefort Dome, as well as in several other domes, notably the Johannesburg Dome. The latter consists of tonalitic, trondhjemitic to granodioritic gneisses (TTG suite) with ages ranging from 3340 to 3114 Ma (Poujol and Anhaeusser 2001) and minor mafic and ultramafic rocks interpreted as remnants of Palaeoarchaean upper mantle or oceanic lithosphere.

The Dominion Group constitutes the earliest supracrustal sequence above the basement rocks. Although not part of the Witwatersrand Supergroup, it reflects first intracontinental basin formation after crustal amalgamation at around 3.1 Ga. The bimodal nature of magmatism in the up to 2250 m-thick volcanic-dominated sequence and a tholeiitic affinity of the mafic rocks therein have been used as evidence of emplacement due to lithospheric thinning (Marsh et al. 1989). Its maximum age is constrained by the youngest age obtained on pre-Dominion basement, i.e. 3086 ± 3 Ma (Robb et al. 1992), and the best available age for the volcanism is 3074 ± 6 Ma (Armstrong et al. 1991). Granite and coeval hornblende gabbro, intersected in drill core through a basement horst on the flank of the Witwatersrand Basin, yielded a U-Pb zircon age of 3062 ± 5 Ma and geochemical/isotopic signatures typical of a volcanic arc setting (Frimmel et al. 2009). They might be related to the Dominion Group volcanic rocks. At its base the group contains a thin basal siliciclastic unit that includes pyritic quartz-pebble conglomerate beds that are of interest in so far as they represent the oldest Witwatersrand-type mineralisation (Dominion Reef). The Au tenor therein is, however, much lower (on average 0.6 g/t), but they constitute a locally economic uranium concentration with a reported resource of 256 Mt @ 0.4 kg/t U_3O_8 (RMG 2015). Rocks of the Dominion Group crop out, or have been intersected in drill core, to the west of the Witwatersrand Basin (Fig. 10.2). Palaeocurrent data consistently indicate a sediment source to the north or northeast (Frimmel and Minter 2002).

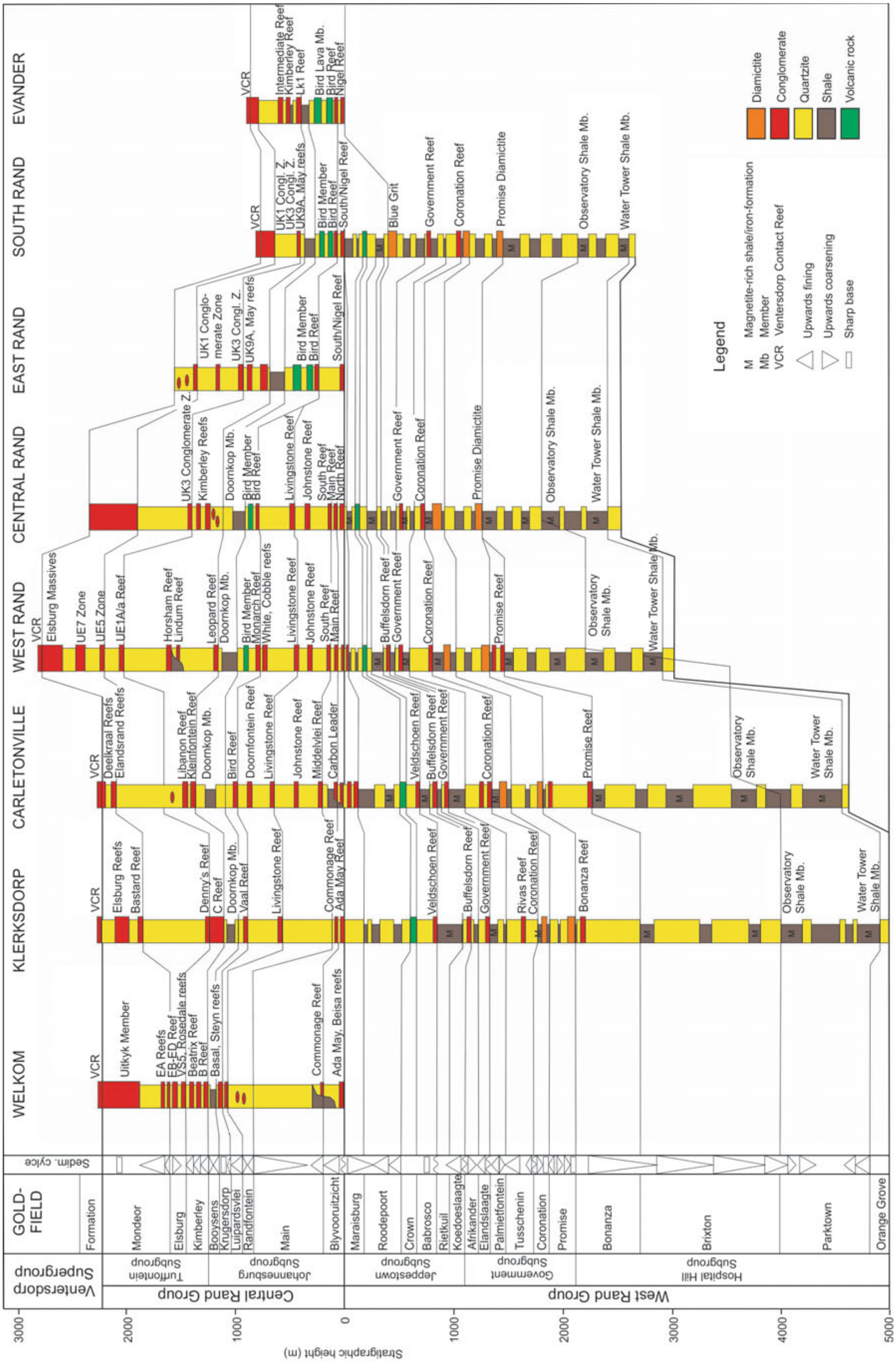

Fig. 10.4 Stratigraphy of the Witwatersrand Supergroup and attempted correlation between the various goldfields. Modified after McCarthy (2006)

10.2.1 West Rand Group

The West Rand Group's lithology is dominated by roughly equal proportions of quartzite and shale. Conglomerate beds are subordinate, largely restricted to the upper parts of the group (Fig. 10.4) and generally distal. Only in one area, west of Klerksdorp, are they proximal in character, and this is the only place where they were mined. Many of the quartzite beds have been interpreted as shallow marine shelf sand accumulations (Eriksson et al. 1981; Winter and Brink 1991). The shale beds are marine, generally rich in iron, with some of them representing proper iron-formation. Three iron-formation marker beds are laterally persistent: (i) in the Water Tower Shale Member, (ii) the Contorted Bed in the Observatory Shale Member, and (iii) the Silverfield iron-formation in the Coronation Formation (Fig. 10.4). A fourth iron-formation bed has been identified in drill core east of Johannesburg within the Promise Formation (Smith et al. 2013). The Promise and Silverfield iron-formations are of particular interest as they overlie diamictite beds that can be correlated with similar marker beds in the Mozaan Group of the Pongola Supergroup (Fig. 10.1) and have become famous as the oldest known glacial deposits in the world (Young et al. 1998). A third diamicite unit, referred to as the Blue Grit Member, at the top of the Afrikander Formation in the South Rand (Fig. 10.4) lacks a corresponding overlying iron-formation, which may be due to erosion prior to deposition of the Jeppestown Subgroup. The contact between the two is a major erosional unconformity.

Noteworthy is the abundance of magnetite as principal Fe-mineral in the marine shale beds as opposed to the dominance of pyrite in the coarser grained, fluvial to shallow marine conglomerates and quartzite beds. The Fe-rich shales have played a major role in sub-surface exploration as magnetic markers (Fig. 10.3) and made possible the development of the Welkom and Evander goldfields in the late 1940s and middle 1950s, respectively, when new aeromagnetic and gravimetric survey technology led to the discovery of the first significant blind ore district. The West Rand Group contains only a single volcanic unit, a basaltic andesite that constitutes the Crown Formation near the top of the group.

10.2.1.1 Hospital Hill Subgroup

The subgroup starts with a thin basal conglomerate and fluvial sandstone (for clarity, the sedimentary protolith names are used here instead of their low-grade metamorphic equivalents) that, over short distance, grade into shallow marine sub-tidal sandstone, fining upwards into silt- and mudstone as well as iron-formation of the Parktown Formation. This sequence is considered to reflect a major transgression of the craton from the southwest. The Parktown Formation is dominated by marine shale with two major iron-formation intercalations, the older one being massive to laminated magnetite-siderite/ankerite-chert bands, the younger one haematite-magnetite rhythmite grading into magnetite-siderite rhythmite. The iron-formation and magnetite mudstone beds are part of upwards coarsening sequences with sharp transgressive upper contacts (Smith et al. 2013). The overlying Brixton Formation contains more sub-tidal sandstone and less mudstone in several upwards coarsening sequences, whereas the Bonanza Formation comprises fluvial sandstone. In the more proximal depositional environments in the west, the latter has few intercalated polymictic, pyritic conglomerate beds (Fig. 10.4). Four cycles of shoreline progradation leading to fluvial deposits can be distinguished in these two formations, each separated by rapid transgressions. Palaeocurrent directions indicate a sediment source area to the north and northwest (McCarthy 2006).

10.2.1.2 Government Subgroup

Great lithological variety marks this subgroup, reflecting repeated cycles of rapid transgression and regression. The base of the subgroup is defined by a laterally extensive diamictite of the Promise Formation (Fig. 10.4). It contains striated clasts and is, together with its correlatives in the Pongola Supergroup as mentioned above, regarded as the earliest glacial deposit recorded so far on Earth. The diamictite is overlain by littoral sandstone and shallow marine ferruginous shale, locally iron-formation, followed by an upwards coarsening sequence into sandstone that is interpreted as resulting from the propagation of a braid-plain at the top of the Promise Formation.

The overlying Coronation Formation consists of shale with a second, intercalated glaciogenic diamictite unit (Kensington Member) that is overlain by iron-formation (Silverfield Member) in the form of finely laminated magnetite-silicate rhythmite (Smith et al. 2013). It reflects rapid marine transgression, only to be followed by a rapid regression that is evident from the disconformable contact with the overlying fluvial conglomerate of the Coronation Reef, followed by fluvial braid-plain quartz wacke, all of which constitutes the Tusschenin Formation (Fig. 10.4).

The Palmietfontein Formation, with a dominance of more or less magnetic marine shale and marine sandstone, indicates renewed marine transgression that was followed again by rapid regression and emergence, evident from the disconformably overlying fluvial conglomerate of the Government Reef at the base of the Elandslaagte Formation. The latter conglomerate is followed by sandstone from a braid-plain environment. Finally, the Afrikander Formation represents a further marine transgression and is made up of mainly marine mud- and sandstone. In the eastern part, it contains a further diamictite bed, the Blue Grit Member. A major hiatus defines the boundary between the Government and Jeppestown subgroups as much of the Afrikander Formation has been eroded prior to Jeppestown deposition.

10.2.1.3 Jeppestown Subgroup

A fluvial conglomerate, the Buffelsdoorn Reef, rests above the basin-wide disconformity at the base of the Koedoeslaagte Formation at the bottom of the subgroup. It is overlain by an upwards fining sequence of littoral sandstone, leading to marine magnetite mudstone of the Rietkuil Formation (Fig. 10.4). The record of the next phase of shoreline progradation is largely absent as the Rietkuil Formation is erosionally truncated by a further disconformity, on top of which follows a conglomerate of the Veldskoen Reef and feldspathic sandstone of the Babrosco Formation (Fig. 10.4). The latter is overlain, across the entire known extent of the West Rand Group, by up to 250 m-thick former lava flows of basaltic andesite of the Crown Formation, followed by sandstone, fining upwards into marine ferruginous, partly magnetic mudstone of the Roodepoort Formation. Much of the Jeppestown Subgroup reflects marine conditions with the basin deepening towards the east. The Maraisburg Formation at the top of the subgroup marks, however, a major regression with propagation of braid-plains from the northwest, leaving behind thick sandstone and subordinate conglomerate deposits (Fig. 10.4).

10.2.1.4 Geochronology and Tectonic Evolution

The maximum age of West Rand Group sedimentation is set by the youngest concordant U-Pb detrital zircon age of 2985 ± 14 Ma from the basal Orange Grove Formation (Kositcin and Krapez 2004). The Rietkuil Formation must be younger than 2931 ± 8 Ma (Kositcin and Krapez 2004) but older than 2914 ± 8 Ma, the age of Crown Formation volcanism (Armstrong et al. 1991). This leaves a maximum time span of some 71 million years for the deposition of as much as 4200 m of sediment (in the Klerksdorp goldfield), that is all of the group up to the Crown Formation, corresponding to a sedimentation rate of 59 m/myr. Considering the existence of several disconformities in the succession, the true maximum integrated sedimentation rate should be even higher. It reflects a combination of initial drowning of the post-Dominion cratonic land surface, followed by repeated cycles of regression and transgression, which at least at Government Subgroup times were largely eustatic. Deepening of the basin towards the south and southeast is deduced from lateral distribution of proximal and distal sedimentary facies (Fig. 10.4). The extent of the West Rand Basin remains unknown but was, in all likelihood, much greater than suggested by the known outcrop and sub-crop of West Rand Group strata. The Mozaan Group of the Pongola Supergroup farther east has been correlated with the West Rand Group (Beukes and Cairncross 1991), thus extending the size of the original basin considerably to the southeast. The tectonic nature of this basin has been a matter of debate. Thermal subsidence may have been responsible for the development of a passive margin to the south(east) of a Mesoarchaean land mass north(west) of today's Witwatersrand, as suggested by uniform palaeocurrent directions from the north, northeast and northwest (Frimmel and Minter 2002) and an upwards decrease in complexity of detrital zircon age spectra (Kositcin and Krapez 2004). The general deepening of the basin, though repeatedly interrupted by eustatic sea level changes, became reversed after extrusion of the Crown Formation lavas. Shoreline propagation and eventual fluvial and braid-plain deposition recorded by the Maraisburg Formation portends the onset of the predominantly continental sedimentation of the Central Rand Group. This development is best explained by a foreland basin superimposed on the older passive margin deposits.

10.2.2 Central Rand Group

The Central Rand Group is unified by the dominance of fluvial to fluvio-deltaic sandstone and conglomerate as opposed to the marine shale-dominated West Rand Group. Principal depositional environments were alluvial braid-plains, especially in the lower Central Rand Group (Els 1998), and alluvial fans, especially towards the top of the group (Kingsley 1987). A further difference to the West Rand Group lies in the sandstone mineralogy. Feldspar is conspicuously absent in the Central Rand Group (Law et al. 1990). The only shale unit of basin-wide extent within the Central Rand Group (Booysens Formation) led Mellor (1917) to a sub-division of the group into two units, now referred to as the Johannesburg and Tuffontein subgroups. Two diamictite units are present within this group, but they differ from those in the West Rand Group by being non-glaciogenic debris flow deposits.

In contrast to the West Rand Group, many of the conglomerate beds in the Central Rand Group are exceptionally rich in gold, with ca. 93% of all the Witwatersrand gold produced so far coming from the Central Rand Group (H.E. Frimmel, unpubl. data). This holds true especially for the proximal areas along the basin edge, where a number of palaeoriver entry points could be mapped out. Most of the conglomerate beds are due to uplift triggered by intermittent tectonic events in the hinterland, followed by periods of tectonic stability and thus low-energy degradation of the conglomerate beds.

10.2.2.1 Johannesburg Subgroup

This subgroup is mainly an aggradational sequence of arenitic fluvial braid-plain deposits. Occasional erosional episodes resulted in widespread peneplanation and thus disconformities that are overlain by conglomeratic placer deposits. Local concentration of gold to ore grade was achieved both by high-energy rivers within incised valleys as well as in thin gravel lags by aeolian transport on exposed surfaces on the interfluves. The latter were also sites of thin layers of carbonaceous material (so-called 'carbon seams'), which represent former microbial mats now consisting of kerogen (Mossman et al. 2008). Several such degradation cycles are distinguished as reflected by the various formations, from bottom to top, the Blyvooruitzicht, Main, Randfontein, Luipaardsvlei and Krugersdorp formations. Each of these typically starts with a basal, in many places auriferous, conglomerate (Fig. 10.4), in one case of (non-glaciogenic) diamictite where argillaceous sediment of the exposed Jeppestown Subgroup became reworked as debris flows into channels cutting through the Main Reef (Martin et al. 1989). From an economic point of view, two degradation episodes stand out, an older one that led to the Main Reefs at the base of the Main Formation (Carbon Leader, Main, South, North, Nigel reefs) and a younger one at the base of the Krugersdorp Formation, especially in the west and northwest of the basin, leaving behind the Basal and Steyn reefs in the Welkom goldfield and the Vaal Reef in the Klerksdorp goldfield (Fig. 10.4). These reefs have constituted the by far richest ore bodies of the Witwatersrand.

Eruption of basaltic lava (Bird Member) during deposition of the Krugersdorp Formation is the only magmatic event recorded in the Central Rand Group and was limited to the northeastern portion of the basin (Fig. 10.4). This was followed by a basin-wide transgression that eventually led to deposition of the only laterally extensive marine shale succession (Booysens Formation) in the Central Rand Group. While fluvial environments clearly dominated in the Central Rand Basin, the Booysens Formation attests to occasional marine incursion in places whereas in others evidence of sub-aerial exposure exists in the form of abundant ventifacts (Minter 1999). Many of the economically important conglomerate bodies take the form of thin laterally extensive sheets, which may be interpreted as result of marine reworking of initially fluvial deposits.

10.2.2.2 Turffontein Subgroup

Deposition of this uppermost subgroup within the Witwatersrand Supergroup set in after a further hiatus at the end of Booysens Formation sedimentation. Progradation of braid-plains led to a coarse-grained sequence with several conglomerate beds, unified as Kimberley Formation. Repeated erosional degradation of these conglomerates left behind deep erosion channels in places and several economic placers (Kimberley Reefs). Further erosional reworking of the older stratigraphy is indicated by the overlying Elsburg Formation which locally contains several sub-economic to economic placers (Fig. 10.4). Towards the end of basin evolution, alluvial fans prograded as the hinterland encroached, leaving behind massive conglomerate and boulder beds (Mondeor Formation) with local placer formation where coarse-grained sediment became reworked at the fan-heads.

10.2.2.3 Geochronology and Tectonic Evolution

Palaeocurrent directions are from all around the current known surface and sub-surface extent of the Central Rand Group (Minter and Loen 1991). Several former river entry points into the basin have been identified thanks to underground exploration for gold for more than a century, because they tend to be sites of maximum gold grades in the fluvial to fluvio-deltaic conglomerates. The positions of the goldfields on the eastern, northern and northwestern to southwestern margin of the area over which the Central Rand Group is known (Fig. 10.2) delineate the former basin margin. This is supported by the spatial distribution of sedimentary facies within a given stratigraphic level, specifically grain size and sorting trends downslope (Minter 1978), all of which point to a deepening of the Central Rand Basin towards the centre of today's known domain occupied by Central Rand Group rocks, which approximates the original size and extent of the depositional basin.

Most of the degradation cycles mentioned above can be explained by syndepositional tectonism in the hinterland, which resulted in a number of largely low-angle unconformities within the Central Rand Group. Major such unconformities exist at the bottom of the Krugersdorp, Booysens, Kimberley and Elsburg formations, with increasing intensity of tilting towards the top of the succession. In the Welkom goldfield, the Elsburg Reefs truncate most of the older strata as they had been up-turned already prior to and during Elsburg deposition (Fig. 10.5). This provides evidence of syndepositional uplift of the hinterland to the west, which involved also progressive unroofing of Neoarchaen granites. The latter is indicated by detrital zircon age spectra (Kositcin and Krapez 2004) as well as changes in sediment chemistry (Nwaila et al. 2017).

The maximum age of sedimentation is given by the age of the Crown Formation volcanic rocks, that is 2914 ± 8 Ma (Armstrong et al. 1991), in the underlying West Rand Group. Further age constraints are from U-Pb detrital zircon ages (Kositcin and Krapez 2004): The bottom of the Central Rand Group is younger than 2902 ± 13 Ma, the Krugersdorp Formation younger than 2872 ± 6 Ma, and the upper Elsburg Formation younger than 2840 ± 3 Ma. Lower age limits of the group are given by a U-Pb age on authigenic xenotime of 2780 ± 3 Ma (Kositcin et al. 2003) and by a U-Pb baddeleyite age from the overlying Klipriviersberg Group, lower Ventersdorp Supergroup, that is

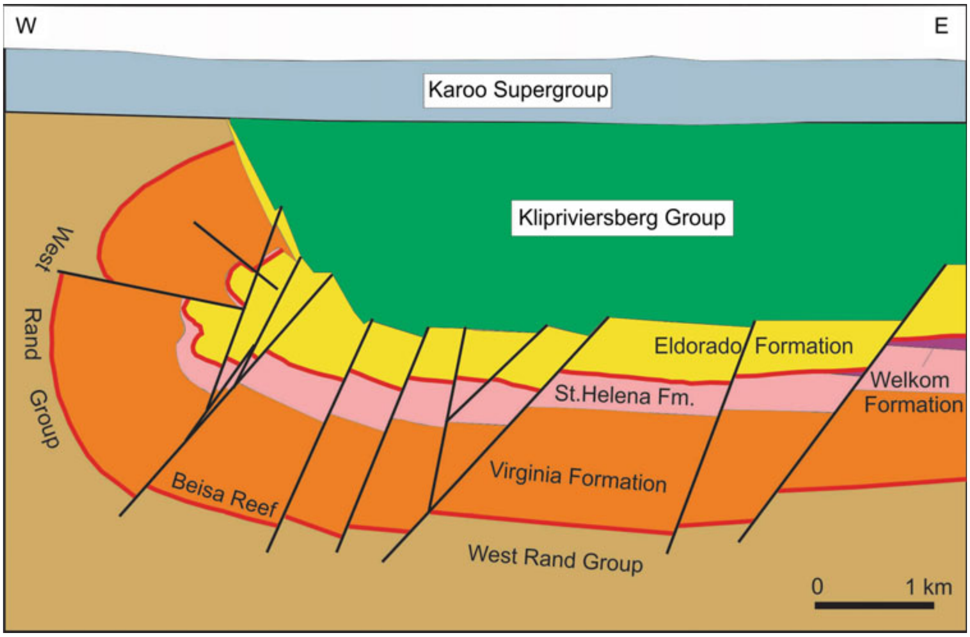

Fig. 10.5 Schematic cross-section through the western margin of the southern part of the Welkom goldfield, showing the up-turning of older Witwatersrand strata prior to and during deposition of the upper Eldorado Formation sediments; note that the Virginia Formation corresponds to the lower Johannesburg Subgroup, St. Helena to the middle Johannesburg Subgroup, i.e. Randfontein to Krugersdorp formations, Spes Bona and Aandenk to Kimberley Formation and Eldorda to the Elsburg and Mondeor formations in Fig. 10.4; from Frimmel and Minter (2002)

2785 ± 1 Ma (Gumsley et al. 2018). Thus, evolution of the Central Rand Basin probably lasted from ca. 2900 to ca. 2785 Ma, which overlaps in time with the Limpopo orogeny, accretion of the Murchison granitoid-greenstone belt to the north and the Kraaipan-Amalia granitoid-greenstone belt to the west (see reviews by Frimmel 2005 and Zeh et al. 2013).

A retroarc foreland setting has been suggested by most workers (e.g. Catuneanu 2001) for several reasons: (i) The numerous low-angle unconformities within the group and syn-sedimentary folding of the older Central Rand Group strata towards the western margin of the basin; (ii) the overall continental composition of most of the sediments and geochemical affinity to arc-derived material (Nwaila et al. 2017); (iii) the large range in palaeocurrent directions from all around the basin (Minter and Loen 1991); (iv) geochemical changes in the sediments, suggesting progressive unroofing of granites in the course of sedimentation (Nwaila et al. 2017); and (v) an overall increase in the complexity of detrital zircon age spectra upsection (Kositcin and Krapez 2004). Taking the above age constraints leaves a time span of some 120 million years, which corresponds to an integrated sedimentation rate of ca. 23 m/myr for the up to 2800 m-thick Central Rand Group. The true sedimentation rate must have been, however, considerably higher, bearing in mind the many hiatuses (of unknown duration) within the group.

10.3 Structure

The structural make-up of the Witwatersrand Basin is, in spite of the scarcity of surface outcrops, comparatively well understood, thanks to many decades of daily underground mapping and surveying by numerous mine geologists (summarised by Dankert and Hein 2010) as well as, more recently, several regional deep seismic (Tinker et al. 2002) and more local 3-D seismic reflection surveys (Manzi et al. 2013). The multitude of data reveals a complex tectonic history with both compressional and extensional forces having shaped the basin to different extents at various times. The seismic data confirmed the unconformity between the West Rand and Central Rand groups as well as the unconformable relation between Witwatersrand and Ventersdorp supergroups, both of which represent periods of tilting and large-scale peneplanation of the old land surfaces.

The above mentioned syn-depositional tectonism in the hinterland during Central Rand Group times, intensifying from Johannesburg to Turffontein Subgroup times, had a profound influence on the structure and sedimentation patterns of the Witwatersrand Basin fill. Within an overall compressional regime, regional uplift of basement domes in the hinterland, development of basin edge faults and uplifted blocks (Fig. 10.6a) became the controlling factors for the source of conglomerates and the location of fluvial channels.

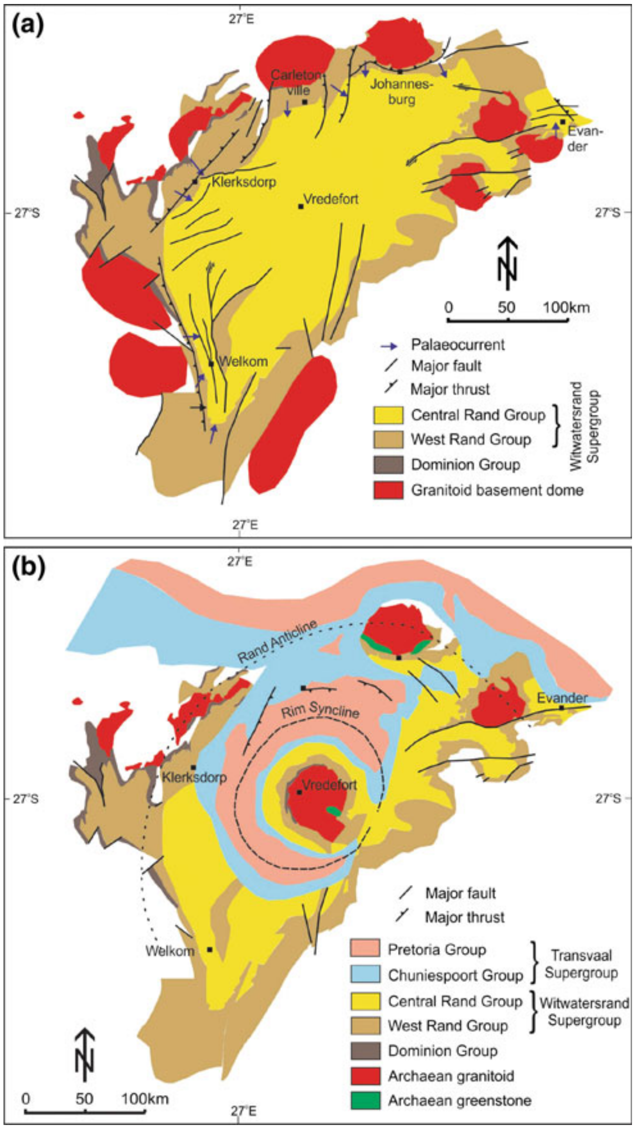

Fig. 10.6 **a** Syn-depositional structures during Central Rand Group sedimentation, showing entry points of major rivers (palaeocurrent directions); **b** Vredefort impact-related structures in the Transvaal and Witwatersrand basins; Ventersdorp and Karoo Supergroup rocks are omitted to better reveal the underlying strata. Modified after McCarthy (2006)

This compressional phase led to first-order folds, thrusts, and reverse faults, especially along the western basin margin, whereas strike-slip movements dominated on the eastern side of the basin (Fig. 10.6a).

After the Central Rand foreland basin had eventually been filled and become subjected to erosion and peneplanation at ca. 2.785 Ga, a major change in the stress field of the central Kaapvaal Craton set in with the outpouring of massive flood basalt and later more evolved volcanic rocks of the Ventersdorp Supergroup. This probably mantle plume-induced episode of volcanism (Crow and Condie 1987) was propelled by extension and heating of the lithosphere, which led to normal faulting and development of graben-and-horst structures across the Witwatersrand Basin. As evident from seismic profiles (Fig. 10.7), these structures are the dominant deformation features in the basin.

10.4 Post-depositional Alteration

Although the Witwatersrand Supergroup has often been considered the best-preserved Mesoarchaean sediment succession in the world, one should not overlook the fact that these ancient rocks experienced some metamorphism as well as hydrothermal alteration. With a maximum total thickness of more than 7 km and further burial beneath some 3 km of Ventersdorp Supergroup and additional several kilometres of Transvaal Supergroup rocks, the lower parts of the former basin fill must have experienced burial metamorphism. The maximum thickness of overburden remains unknown. Integrating the maximum thicknesses reported for the various units of the Transvaal Supergroup yields ca. 16 km but the thickest portions of each unit were never stacked on top of each other in the same area. Furthermore, major erosion on top of the Witwatersrand and the Ventersdorp supergroups would have removed large portions of older stratigraphy prior to the deposition of younger strata. Further burial beneath the Mesozoic Karoo Supergroup rocks probably did not add to the overall maximum metamorphic grade because it occurred after parts of the Palaeoproterozoic succession had already been removed by erosion. Although we do not know the exact maximum depth to which the Witwatersrand Supergroup rocks had been buried, phase relations indicate lower greenschist-facies conditions (Wallmach and Meyer 1990; Frimmel 1994). Tectonic shortening in the course of thrusting of the Limpopo Belt's Southern Marginal Zone onto the Kaapvaal Craton between 2690 and 2670 Ma affected at least the northern parts of the Witwatersrand Basin. The emplacement of the world's largest layered intrusive complex, the 2054 Ma Bushveld Complex, to the immediate north of the Witwatersrand Basin must have had at least some thermal effect on the latter's fill. Of probably even greater consequence was the 2023 Ma Vredefort impact that left behind a 90 km-wide domal structure in the middle of the known area of Central Rand Group rocks. The original diameter of the impact structure has been modelled from geophysical data as 250–280 km, which corresponds closely to the size of the Witwatersrand Basin (Henkel and Reimold 1998). An impact-induced basin-wide network of fractures and low-angle thrusts, now partially filled with pseudotachylyte, created a secondary permeability long after primary permeability of the sedimentary rocks had been eliminated by diagenesis and metamorphism. This made it

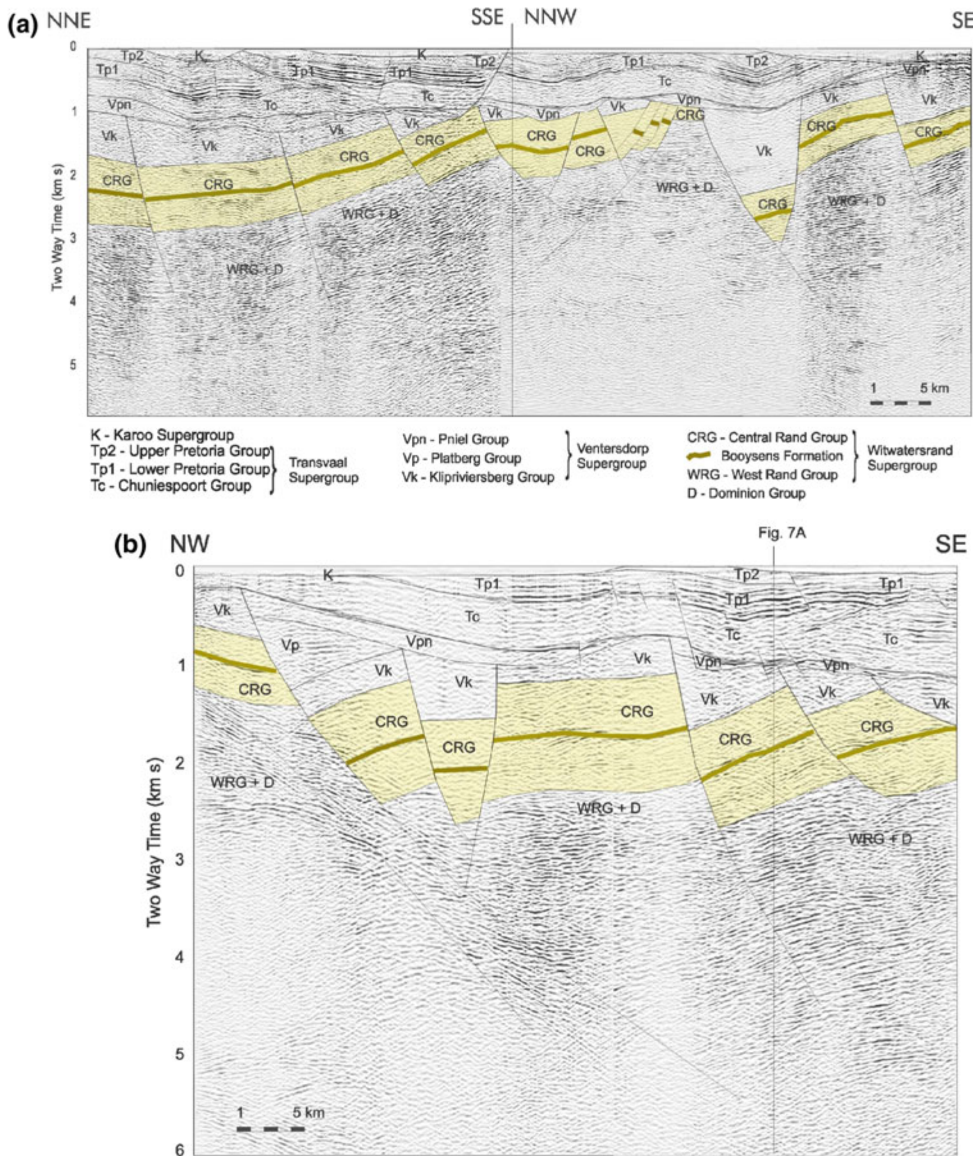

Fig. 10.7 Stacked and migrated reflection seismic profiles through parts of the Witwatersrand Basin with stratigraphic interpretation from Tinker et al. (2002); highlighted are the Central Rand Group and the Booysens Formation shale in the middle of that group; for lines of sections see Fig. 10.2

possible for fluids to circulate throughout the former basin fill—at least for a short time—and cause hydrothermal alteration along the fractures (Frimmel et al. 1999). Although the impact cannot have anything to do with the exceptional gold endowment of the Witwatersrand rocks (the mineralisation took place some 900 million years before the impact occurred), it played a decisive role in the preservation of these Archaean sedimentary rocks. The infolding of the Witwatersrand strata in a concentric synclinorium around the Vredefort Dome (Fig. 10.6b) helped to preserve them from later erosion, thus providing an explanation for the apparently fortuitous position of the world's largest known impact structure in the centre of the area of preserved Central Rand Basin fill (McCarthy 2006).

The net result of the above events was generally low-grade metamorphism, reaching even higher grade in the lower parts of the basin fill, which are now exposed up-turned to almost vertical position along the collar of the impact-induced Vredefort Dome (Gibson and Wallmach 1995). The generally low metamorphic grade, quantified by thermodynamic modelling of observed phase relationships (Wallmach and Meyer 1990; Frimmel 1994; Phillips and Law 1994) as 350 ± 50 °C at ca. 3 kbar, seems fairly uniform across the former basin. This should not distract, however, from the fact that peak metamorphic conditions were most likely achieved not at the same time throughout the basin but at different times, depending on position (Frimmel 1997). Various tectono-metamorphic events along the margins of the Kaapvaal Craton after the emplacement of the Bushveld Igneous Complex had, by and large, only very little influence on the Witwatersrand Basin fill and are not further considered here.

Evidence of hydrothermal alteration is prevalent throughout the Witwatersrand Basin fill, especially in the more competent rock types that are prone to fracture-controlled fluid percolation, such as quartzite and conglomerate. In contrast, less competent shale beds remained barely affected. In general, the observed metamorphic mineral assemblages, especially the abundance of pyrophyllite, indicate largely acidic fluid conditions. This has led some workers to argue for basin-wide H^+-metasomatism that also supposedly caused the introduction of gold into the Witwatersrand strata (Barnicoat et al. 1997). As opposed to fluid infiltration from a source external to the basin as suggested by the latter authors and others (Phillips and Powell 2011), the acidic conditions could be also due to diagenetic flow of groundwater towards the basin centre, following a hydraulic gradient that had been established by uplift along the basin margin. With increasing burial, maturation of organic matter and release of H^+ by dehydration reactions could have lowered the pH, thus leading to the dissolution of detrital feldspars. Such a development of groundwater and formation water could explain the lack of detrital feldspar in the Central Rand Group and the observation, based on geochemical data, that the arenitic rocks remained largely isochemical, except for the mobilisation of potassium (Sutton et al. 1990). It is, however, more likely that, at least in parts, geochemical alteration of the predominantly arenitic rocks is a palaeo-weathering effect. A wealth of geochemical analyses of arenitic units, across the Central Rand and subordinately from the West Rand Group, document progressive removal of Ca and Na (related to plagioclase weathering), followed by removal of K (due to K-feldspar weathering) from the average composition of Archaean upper continental crust (Frimmel 2005). The Chemical Index of Alteration (CIA), as defined by Nesbitt and Young (1982), of the various sedimentary units varies greatly with stratigraphic depth and reaches particularly high values in the Central Rand Group (Frimmel 2005). Peaks in CIA are distributed not randomly but systematically in the footwall of old erosion surfaces. This strongly points at intense chemical weathering on the old land surfaces that were exposed in Central Rand Group times with alteration of detrital feldspar to kaolinite (and similar clay minerals), which subsequently turned into pyrophyllite during metamorphism (Wallmach and Meyer 1990; Frimmel 1994).

Chemical weathering over tens of metres into the footwall below conglomerate beds (palaeoerosion surfaces) notwithstanding, there is also evidence of more or less bedding-parallel fluid flow along low-angle thrust planes within some of the conglomerate beds (Jolley et al. 1999). A prime example is the post-Witwatersrand Ventersdorp Contact Reef, an up to several metres thick fluvial conglomerate with minor quartzite intercalations at the base of the Ventersdorp Supergroup. It forms the richest ore body outside of the Witwatersrand Supergroup. Capping by impermeable flood basalt of the 2.785 Ga Klipriviersberg Group enabled focusing of post-depositional fluids that emanated from the underlying Witwatersrand strata into this conglomerate unit. This caused initially considerable potassic alteration along the conglomerate and into the overlying metabasalt as well as the underlying quartzitic footwall over a vertical distance of a few metres, followed by more channelled chloritisation along the conglomerate and the immediate hanging and footwall (Gartz and Frimmel 1999). Thus, throughout the Witwatersrand, alteration phenomena in the coarser grained sedimentary units comprise a combination of large-scale, more or less stratiform, deep chemical weathering below palaeoerosion surfaces and, locally, highly focused post-depositional potassic alteration (sericitisation) and chloritisation along some of the conglomerate beds. The latter also led to the formation of quartz veins (and calcite veins within the overlying Klipriviersberg metabasalt), which are locally mineralised, thus testifying to some remobilisation of initially conglomerate-hosted ore components. It should be noted, however, that the overall amount of quartz veins across the Witwatersrand strata is surprisingly low, considering the sheer amount of SiO_2 in the basin fill and the general low metamorphic grade.

Witwatersrand shales show little evidence of hydrothermal alteration, except in the immediate vicinity of faults, dykes, veins, and along contacts with adjacent more permeable arenitic rocks. They retained mass-independent sulphur isotope signals (uniform negative $\Delta^{33}S$ and largely negative $\delta^{34}S$ ratios) that are indicative of Mesoarchaean atmospheric sulphur speciation (Farquhar et al. 2007)—signals that would not survive significant post-depositional hydrothermal overprint (Hofmann et al. 2009; Guy et al. 2010). Consequently, the composition of marine Witwatersrand shales can be used as proxy of provenance and intensity of chemical weathering in the source areas. Geochemical data of such shales reveal high CIA values and thus provide evidence of intense chemical weathering in their source areas (Nwaila et al. 2017).

10.5 Sediment Provenance

Most of the Witwatersrand conglomerates have a pebble assemblage that is strongly dominated by quartz, much of which is derived from granite and pegmatite (55%) and from greenstone-hosted vein quartz and chert (45%), as indicated by oxygen isotope data (Vennemann et al. 1992, 1995). Volumetrically minor clast types are quartz porphyry (3%) and metamorphic clasts (2%). Exceptions are the Steyn Reef in the Welkom goldfield with up to 30% porphyry clasts and the Kimberley Reef in the Evander goldfield with as much as 50% chert clasts (Tweedie 1986). A mix of (ultra)mafic and felsic source rocks is indicated by the heavy mineral populations, which include detrital chromite and PGE-minerals from former and detrital zircon, uraninite, columbite, molybenite and cassiterite from latter sources, respectively (Feather and Koen 1975). Such a lithological mix in the hinterland is also indicated by the geochemistry of the arenitic fraction, which reflects variable degrees of chemical weathering of mafic to felsic source rocks (Frimmel 2005). The same applies to shale beds in the West and Central Rand groups (Nwaila et al. 2017). Several elements, typically concentrated in detrital phases, can be used as proxies for the relative contribution of certain source rock types to the sediment mix. Examples are Zr for felsic sources and Cr and Sc for mafic sources. Furthermore, a negative correlation between Ni and total organic carbon (TOC) attests to the Ni budget in the pelitic sediments to be principally controlled by the proportion of mafic/ultramafic rocks in the hinterland (Nwaila et al. 2017).

As mafic and ultramafic rocks are more magnesian, pelitic sediments from such source rocks have a higher X_{Mg} (= Mg/(Mg + Fe) ratio. Thus, using the ratios of elements typical of felsic and mafic/ultramafic rocks, respectively, the relative proportion of principal source rock types for different stratigraphic levels across the Witwatersrand Supergroup have been calculated (Nwaila et al. 2017), according to which the lowermost West Rand Group sediments were derived from granitic sources, with a roughly equal proportion of TTG and granitic source in the upper Hospital Hill Group, again an almost exclusively granitic source for the lower Government Subgroup, changing to predominantly TTG and minor granitic sources for the upper part of that subgroup. The Jeppestown Subgroup reflects a major change in sediment provenance towards a mix of TTG and mafic source. Across the Johannesburg to lower Turffontein subgroups, mafic rocks played a particularly dominant role as source, whereas towards the top of the latter group, TTGs and granitic sources became dominant again. Significant deviations from this general trend can be observed within a given stratigraphic unit between different goldfields. For example, the provenance of the Booysens Formation shale in the Welkom goldfield was felsic whereas farther north(east) it was predominantly mafic. At a given locality, the proportion of mafic to felsic detrital sediment input can change substantially within a single formation, e.g. Zr/Ni increasing from < 0.2 (mafic) to > 0.8 (felsic) from the bottom to the top of the Booysens Formation shale (Nwaila et al. 2017). Detrital zircon ages in the Witwatersrand metasedimentary rocks mirror the age distribution of the surrounding Archaean granitoid-greenstone belts (Frimmel et al. 2005; Koglin et al. 2010b), thus strongly confirming that these belts acted as principal source domains for the Witwatersrand sediments.

10.6 Mode of Mineralisation

Most of the gold occurs, together with other heavy minerals of undoubtedly allogenic nature, in fluvial conglomerates, pebbly arenite and pebble lag surfaces associated with trough cross-bedded quartz arenite (Fig. 10.8). The orebodies are typically bounded by a basal degradation surface, usually an angular unconformity, and an upper planar bedding surface that is due to either aeolian deflation (Minter 1999) or shoreline encroachment (Buck and Minter 1985). Thicker (a few metres) units represent multichannel sequences with the heavy minerals, including gold, being concentrated along the basal degradation surface of each graded bed. Elsewhere, a few centimetres-thin pebble lags define degradation surfaces that can contain very high gold grades (Frimmel et al. 2005). Furthermore, elevated heavy placer mineral contents are found at the base of clast-supported oligomictic to loosely packed conglomerates, rarely in immature debris flow deposits (Minter et al. 1988). The contacts of the ore bodies are always sharp with regard to ore grade. Whereas the Au grade within the conglomerates can attain several grams to tens of grams per tonne, it drops by a few orders of magnitude across the boundaries, be it an unconformity or bedding plane, against the arenitic footwall and hanging wall.

In addition, a considerable proportion of gold is hosted by millimetre- to centimetre-thick kerogen layers, locally referred to as 'carbon seams' (Fig. 10.9), which in some instances, such as the Carbon Leader Reef, hosted as much as 70% of the entire gold (Hallbauer and Joughin 1973). Such gold-rich kerogen mats occur essentially in the lower Central Rand Group, good examples being the mentioned Carbon Leader, the Basal Reef or the Vaal Reef.

For decades it has been repeatedly observed that, under the microscope, much of the gold occurs in late paragenetic textural positions (Ramdohr 1958), together with

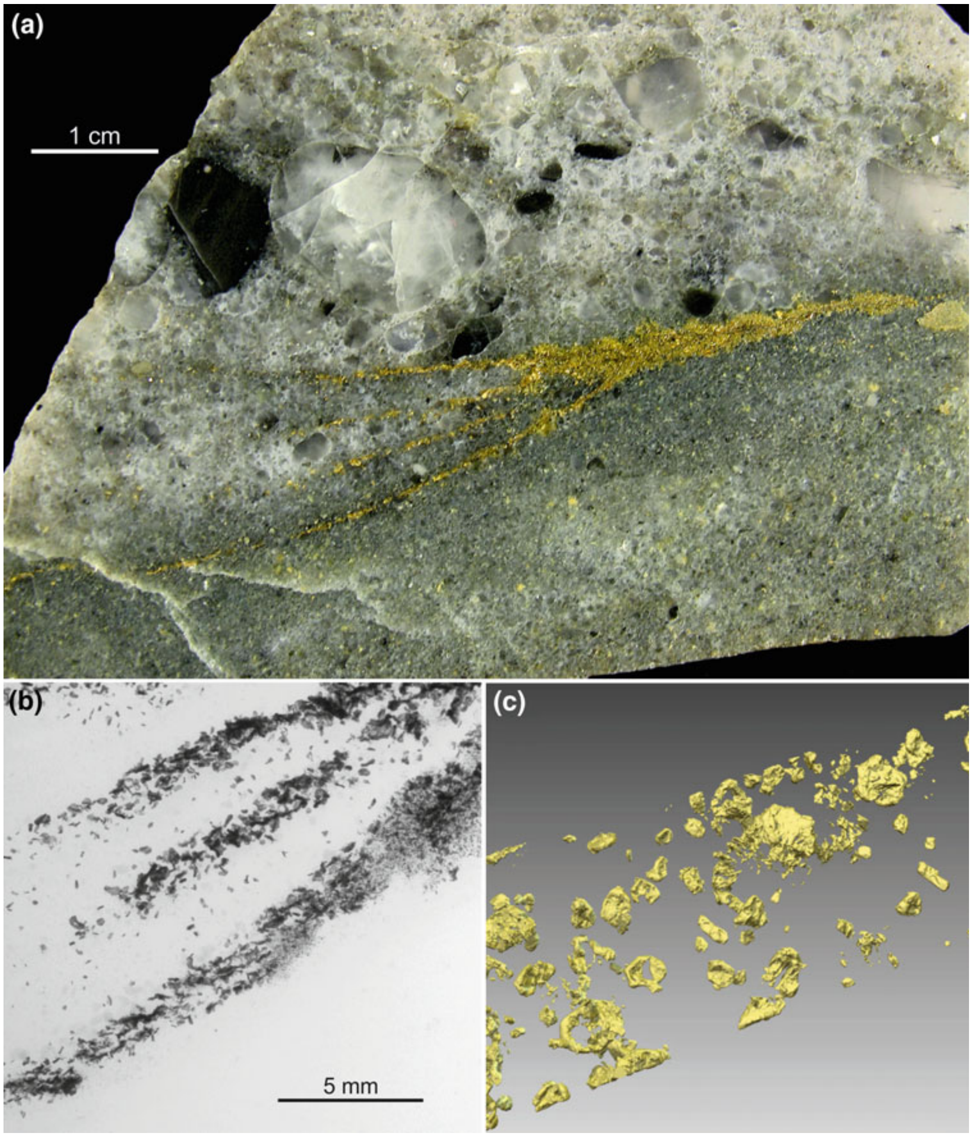

Fig. 10.8 **a** Gold concentrated along crossbeds in pebbly quartz arenite at the base of the Basal Reef, Free State Geduld mine, Welkom goldfield; **b** Attenuation radioscopic X-ray image of gold particles along the crossbeds; **c** 3-D detail of the middle of radiograph shown in (**b**); width of photo is 4 mm; from Hölzing et al. (2015)

hydrothermal bitumen, metamorphic chlorite (Gartz and Frimmel 1999), pyrophyllite (Barnicoat et al. 1997), or as inclusions in euhedral, secondary pyrite (Frimmel 2005). This type of gold is, without doubt, the product of precipitation from hydrothermal/metamorphic fluids, which has led several researchers to suggest an overall epigenetic, hydrothermal origin of the gold (e.g. Phillips and Law 2000; Phillips and Powell 2011). It should be noted, however, that the above late paragenetic position of the gold does not provide any indication as to the distance of hydrothermal gold transport, whether the gold was introduced into the conglomerates from an external source far away or whether it represents locally remobilised placer gold within the conglomerates. Several observations speak for the latter case. Some of the gold occurs in textural positions and morphological forms that leave little doubt as to their detrital nature. These are mechanically rounded, spheroidal to toroidal particles that are associated with other heavy minerals as placer concentrates, a prime example of which is illustrated in Fig. 10.8. With typical diameters of some 100–150 µm they can be regarded as micronuggets. Larger, proper nuggets are notably absent.

In spite of the exceptional endowment, visible gold is rare in the Witwatersrand. It is found either as placer concentrate (Fig. 10.8) or as secondary, hydrothermal gold in quartz veins, micro-shears and fractures. Gold in the latter, cross-cutting features is typically confined to domains in the immediate vicinity of gold-rich conglomeratic reefs. It thus reflects mobilisation of gold from the conglomerate beds into whatever cross-cutting, fluid-filled feature, whereas nowhere is an example known that would illustrate dispersion of gold from a cross-cutting feeder channel into the siliciclastic wall rocks. Although various epigenetic-hydrothermal models, analogous to orogenic gold models, have been suggested for decades by some workers (e.g. Phillips and Powell 2011) as prospective guide for future exploration, not a single cross-cutting ore body has been mined or discovered over the century-long mining history of the Witwatersrand.

Besides gold, U-minerals, pyrite and hydrocarbons are important constituents of the ore whose genesis has been a matter of debate as much as that of the gold itself. Their mode of occurrence has direct bearing on our understanding of Witwatersrand gold genesis. The U-minerals can be locally of economic significance, with some 28 mines having been producers of uranium in the past, mainly from the Bird Reefs in the West Rand and Klerksdorp goldfields (Tucker et al. 2016). Uraninite is the by far most abundant U-mineral in the gold fields and occurs mainly as semi-rounded, millimetre-sized grains whose chemical composition speaks for an evolved granitic/pegmatitic provenance but against a hydrothermal origin (Frimmel et al. 2014). The latter study also revealed systematic differences in the trace element distribution within uraninite populations from different former river systems (Basal and Steyn placers, Welkom goldfield), all of which leaves little doubt on the detrital nature of these grains. Minute, in places sub-microscopic U-minerals, predominantly brannerite, subordinately secondary uraninite, are doubtlessly the product of hydrothermal mobilisation of some of the uranium by post-depositional fluids (Depiné et al. 2013; Fuchs et al. 2016). The variety of pyrite types is even wider: pre-, syn- and post-depositional types have been distinguished, initially merely on morphological grounds (Hallbauer 1986), later on also based on sulphur isotopic evidence (England et al. 2002; Hofmann et al. 2009) and trace element data (Koglin et al. 2010a; Guy et al. 2010; Agangi et al. 2015). These studies document the presence of (i) rounded, mechanically abraded, evidently detrital pyrite derived from hydrothermal veins, volcanic-hosted massive sulphide deposits, sulfidised Fe-oxides or black shales; (ii) concentrically laminated pyrite rich in trace elements, including Au, that formed within the wet sediment and/or during early diagenesis, and (iii) epigenetic-hydrothermal pyrite in the form of euhedral cubes or overgrowths around the previous two types. Detrital pyrite is the by far most abundant type. Locally, some reefs, such as the Ventersdorp Contact Reef, seemingly contain more euhedral pyrite, but careful examination by etching revealed that many of the euhedral pyrite grains represent hydrothermal overgrowths around detrital pyrite cores (Gartz and Frimmel 1999). Repeated mechanical reworking of ore constituents is beautifully illustrated by a mechanically rounded polymictic pyritic pebble with inclusions of rounded uraninite, rounded pyrite, rounded pyrrhotite and rounded chromite all of which are bound together by secondary interstitial pyrite (Fig. 10 in Tucker et al. 2016).

Hydrocarbons occur in two principal forms, the above-mentioned stratiform ‘carbon seams’ on top of erosion surfaces and millimetre- to centimetre-sized nodules (so-called ‘flyspeck carbon’). Although some workers (e.g. Gray et al. 1998; Drennan and Robb 2006; Fuchs et al. 2016) argued for both of these being products of migrating oils (thus representing pyrobitumen), field relations and isotopic data argue against such an interpretation. Whereas the nodules are without doubt pyrobitumen and related to post-depositional fluid flow, as they also occur within quartz veins, the ‘carbon seams’ are interpreted as former microbial mats as originally suggested by Hallbauer (1975). This is supported by a wealth of very delicate sedimentary structures defined by the ‘carbon seams’, and field evidence of intraformational sedimentary reworking of such seams (Mossman et al. 2008; Frimmel 2014). In addition, C isotope data (Spangenberg and Frimmel 2001) reveal a lack of fractionation across the range of *n*-alkanes, which argues against any long-range mobilisation of bitumen (Frimmel and Hennigh 2015). The texture of the ‘carbon seams’ has been affected, however, by post-depositional strain, and original microbial microstructures were lost.

An intimate spatial association of uraninite and hydrocarbons, evident in many reefs, can be explained by three independent processes, that is (i) microbial growth on pebble beds rich in heavy detrital minerals, including uraninite, (ii) polymerisation and cross-linking of liquid hydrocarbons on the surface of detrital uraninite grains (Schidlowski 1981), and (iii) remobilisation of U by carbonic fluids giving rise to secondary U-minerals intergrown with pyrobitumen (Fuchs et al. 2016). A positive correlation exists between Au and U as expected for elements principally housed in co-existing detrital minerals, but in most areas this correlation is relatively weak because of short-range dispersion of both elements by post-depositional fluids (Frimmel and Minter 2002). Similarly, a positive correlation exists between Au and Zr in some instances. A larger data set, however, reveals many conglomerate samples rich in Zr and poor in Au (as expected for heavy mineral concentrates that lack detrital gold) but, with a single exception, no sample that is rich in Au and poor in Zr, as would be expected for hydrothermal systems in which Zr is typically not very mobile (Frimmel et al. 2005).

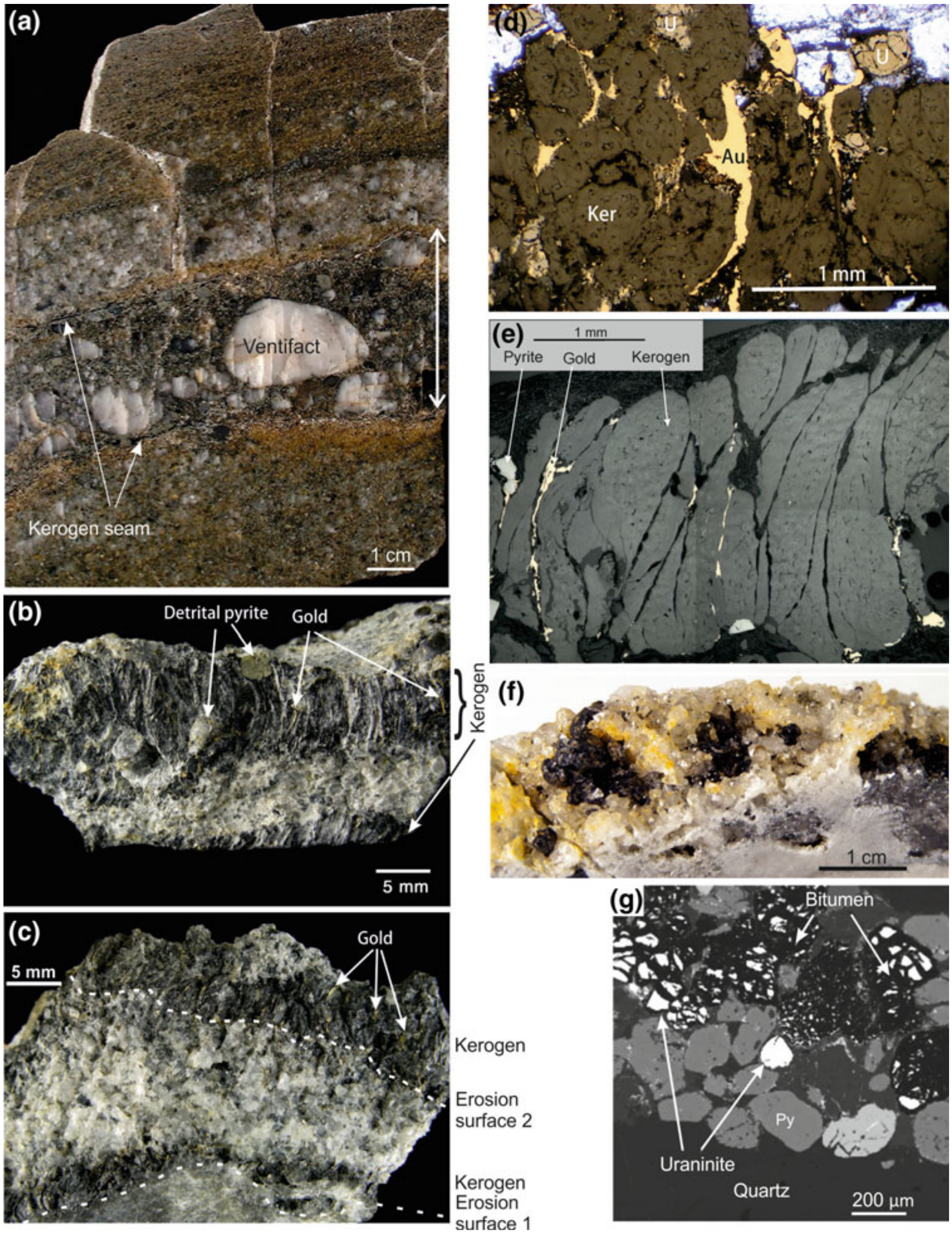

Fig. 10.9 Mode of hydrocarbon occurrence in Witwatersrand rocks: **a** Thin kerogen seams on scour surfaces at bottom of pebble lags, Steyn Reef, President Steyn mine, Welkom goldfield; pebble lag represents an aeolian deflation surface (vertical double arrow) as indicated by ventifact; **b**,**c** Gold-rich kerogen seams with interstitial heavy minerals (pyrite) at the base of the Vaal Reef, Stilfontein mine, Klerksdorp goldfield; **d** microphotograph under combined transmitted and reflected light of kerogen seam (Ker) rich in platy gold (Au) and intercalated detrital uraninite (U) from base of the B-Reef, Tshepong mine, Welkom goldfield; **e** reflected light microphotograph of columnar kerogen with gold platelets between columns from base of Carbon Leader, West Driefontein mine, Carletonville goldfield (from Frimmel and Hennigh 2015); **f** pyrobitumen globules (black) on drusy quartz vein, Ventersdorp Contact Reef, Tau Lekoa mine, Klerksdorp goldfield; **g** back-scatter electron image of pyrobitumen (black) enclosing broken-up detrital uraninite fragments (white) in quartz-pebble conglomerate, note that some uraninite (rounded grain in the middle) is not enclosed by pyrobitumen, Vaal Reef, Great Noligwa mine, Klerksdorp goldfield; from Depiné et al. (2013)

10.7 Towards a Holistic Metallogenetic Model

A purely epigenetic, hydrothermal model for the Witwatersrand gold can be discarded for many reasons, including the presence of evidently detrital micronuggets (Fig. 10.8), the strong sedimentological control on ore grade and the lack of cross-cutting ore bodies. A purely syngenetic placer model defies, however, the observation of much of the gold occurring in late paragenetic textural positions. This apparent contradiction has been overcome by the currently favoured 'modified placer model', according to which placer mineralisation was followed by mobilisation of ore components, including gold, by post-depositional fluids (Robb and Meyer 1991; Frimmel et al. 1993). It should be emphasised, however, that the mobilisation of gold took place, in most instances, over only very short distances of a few millimetres to maybe metres, largely confined to within the original host conglomerate beds, and is thus of little economic significance. While consensus on this genetic model seems to be reached, the ultimate question as to the source of all the implied detrital gold in the Witwatersrand Basin has remained unresolved and posed, in fact, the possibly biggest challenge to a (modified) placer model.

Numerous discrete sources have been suggested in the past, foremost greenstone-hosted auriferous vein deposits in the hinterland. Apart from a gold chemistry that is at odds with a hydrothermal source (Witwatersrand gold contains orders of magnitude more Os than any other hydrothermally derived gold analysed so far), simple mass balance excludes such a source (Frimmel 2014). Other suggestions, such as hydrothermally altered granites in the hinterland or syn-depositional exhalites along the basin margin, had to be discarded when the granite alteration was found to be younger than the gold mineralisation in the Witwatersrand and due to a lack of any geological evidence of the suggested exhalites along the basin margin, respectively. No kind of discrete gold deposit in the Mesoarchaean hinterland can explain the huge amounts of postulated detrital gold in the Central Rand Basin. This leaves only the mobilisation of background concentrations of Au from the hinterland or underlying crust as alternative. Such large-scale leaching could have been achieved by regional metamorphic devolatilisation, as suggested by Phillips and Powell (2011), but this would imply an overall epigenetic gold mineralization, which has been discarded as likely genetic model (see above). Large et al. (2013) proposed pyritic shales farther down in the Witwatersrand stratigraphy as important source of gold (and pyrite) in the Central Rand Group conglomerates, but problems in both mass balance and timing of sediment deposition, mineralisation and fluid flow render this hypothesis unlikely. The only remaining option is syn-depositional leaching of background Au by surface waters.

Reconstruction of the likely environmental conditions during the Mesoarchaean, combined with thermodynamic modelling, led Frimmel (2014) and, independently, Heinrich (2015) to suggest that gold solubility in river waters at that time was orders of magnitude greater than today. This, combined with a period of intense chemical weathering under an aggressive acid atmosphere, enabled craton-wide leaching of gold from the granitoid-greenstone terrains in the hinterland and a tremendous flux of Au, largely in dissolved form, off the land into the ocean. Thus the entire Mesoarchaean land surface becomes a potential gold source. Only a small portion of all this gold was needed to be trapped to form the first major gold deposits. And the most effective trap was constituted by early microbial mats in coastal wetlands, shallow marine to littoral positions, and on mudflats along rivers. The geological evidence of the oldest, very rich ore bodies in the Witwatersrand (e.g. Carbon Leader) attests to the efficiency of such microbial mats in fixing gold from the surrounding river water or seawater. This could have been achieved either by reduction on the organic surface as suggested by Heinrich (2015) or by oxidation in an overall O_2-deficient atmosphere, triggered by the first O_2-producing photosynthesisers, most likely cyanobacteria, as suggested by Frimmel (2014). Whatever the redox-reaction might have been, microbial fixation of large amounts of gold is likely and, considering the extremely low preservation potential of such microbial mats, provides an ideal source for the detrital gold in the Witwatersrand conglomerates (Fig. 10.10). It also explains the lack of proper larger nuggets because of the generally very small size of the delicate gold filaments and platelets that drape kerogen columns in the 'carbon seams'.

All in all, the exceptional gold endowment of the Witwatersrand is now seen as the product of the fortuitous interplay of changes in atmospheric conditions, chemical weathering rate, abundance of reduced S-species in the meteoric environment, and the evolution of life forms, specifically the emergence of photosynthesising microbes at around 2.9 Ga. It is the product of a unique window of opportunity, never to be repeated again, when the conditions were ideal for continent-wide leaching and large-scale trapping of gold in and around coastal environments. Mechanical reworking of the gold-bearing microbial mats led to initially very rich placer deposits (Fig. 10.10).

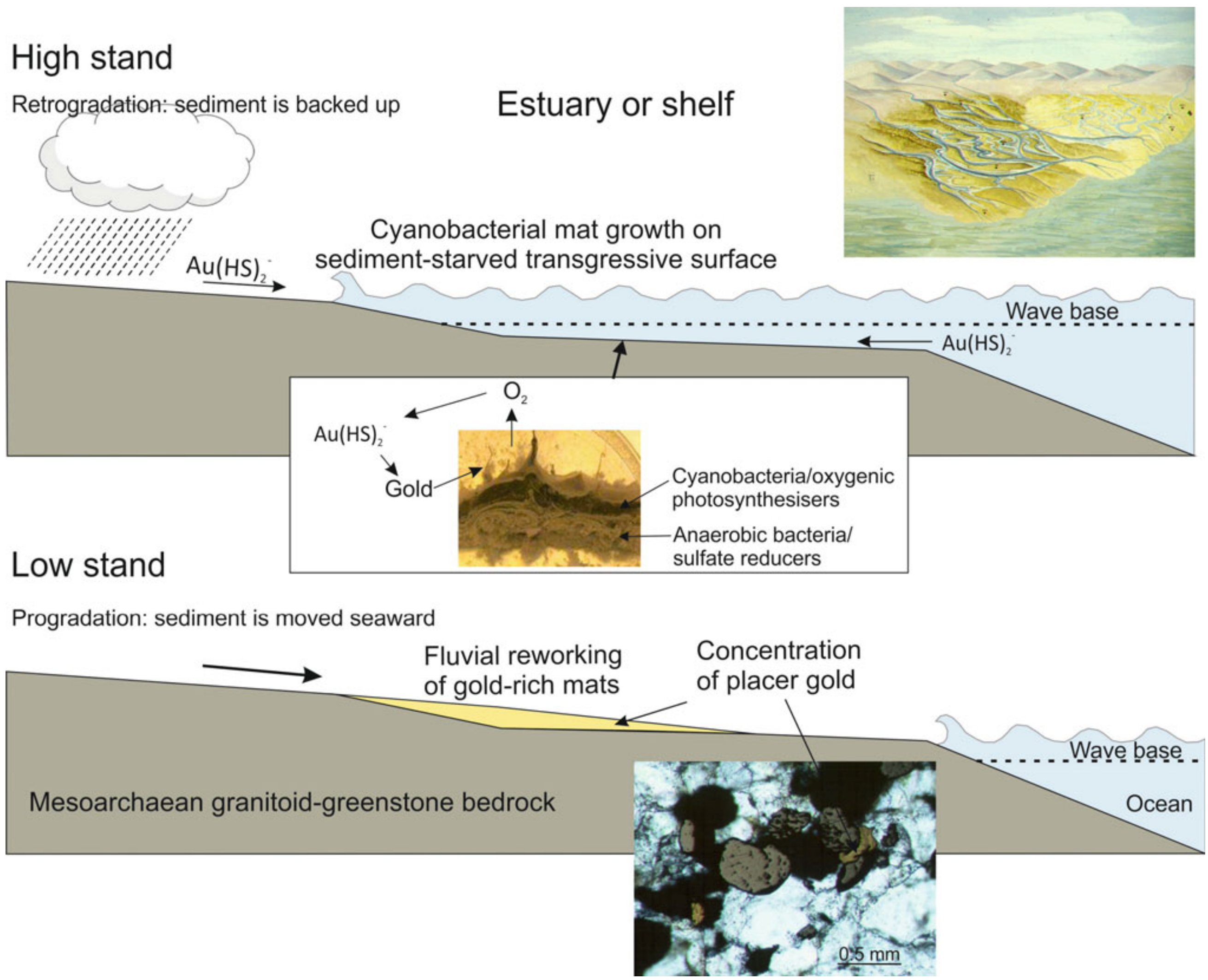

Fig. 10.10 Schematic cartoon illustrating the two principal gold concentration mechanisms in the Mesoarchaean Central Rand Basin: (i) microbial gold fixation from $Au(HS)_2$—bearing meteoric waters and shallow seawater and (ii) sedimentary reworking of that gold by rivers

The potential to form such rich placers diminished over time when less and less of the microbial mats and early placers became available for erosion (Frimmel 2018).

The above processes of gold accumulation were surely not restricted to the Kaapvaal Craton but should have operated on all Mesoarchaean cratons and their margins. In most areas, the corresponding sediments became reworked during subsequent erosion or tectonic, orogenic, magmatic or metamorphic overprints. The uniqueness of the Witwatersrand is rooted in its exceptional preservation, which is owed to the incidental combination of three geological factors: (i) the Witwatersrand sediments became covered to a large extent by a thick pile of extremely competent, erosion-resistant basalt (Ventersdorp Supergroup), (ii) the subsequent deformation into bowl-shape by the Vredefort impact and further protection by a likely veneer of hardened impact melt, and (iii) its position in the middle of one of the oldest and most buoyant cratons where it largely escaped later orogenic overprints.

Acknowledgements Numerous mining companies and their mine geologists are thanked for providing access to underground workings and samples over a > 25 years research period. W.E.L. Minter is thanked for passing on to me valuable collections of rock samples from old mines that are not accessible anymore. Parts of the thoughts expressed in this paper are based on research funded by the South African National Research Foundation (NRF) and the Deutsche Forschungsgemeinschaft (DFG grant FR2183/3).

References

Agangi A, Hofmann A, Rollion-Bard C, Marin-Carbonne J, Cavalazzi B, Large R, Meffre S (2015) Gold accumulation in the Archaean Witwatersrand Basin, South Africa—Evidence from concentrically laminated pyrite. Earth-Sci Rev 140:27–53

Armstrong RA, Compston W, Retief EA, William LS, Welke HJ (1991) Zircon ion microprobe studies bearing on the age and evolution of the Witwatersrand triad. Precambr Res 53:243–266

Barnicoat AC, Henderson IHC, Knipe RJ, Yardley BWD, Napier RW, Fox NPC, Kenyon AK, Muntingh DJ, Strydom D, Winkler KS, Lawrence SR, Cornford C (1997) Hydrothermal gold mineralization in the Witwatersrand basin. Nature 386:820–824

Beukes NJ, Cairncross B (1991) A lithostratigraphic-sedimentological reference profile for the late Mozaan Group, Pongola Sequence: application to sequence stratigraphy and correlation with the Witwatersrand Supergroup. S Afr J Geol 94:44–69

Buck SG, Minter WEL (1985) Placer formation by fluvial degradation of an alluvial fan sequence: the Proterozoic Carbon Leader placer, Witwatersrand Supergroup, South Africa. J Geol Soc London 142:757–764

Catuneanu O (2001) Flexural partitioning of the late Archaean Witwatersrand foreland system. Sed Geol 141–142:95–112

Crow C, Condie KC (1987) Geochemistry and origin of late Archaean volcanic rocks from the Rhenosterhoek Formation, Dominion Group, South Africa. Precambr Res 37:217–229

Dankert BT, Hein KAA (2010) Evaluating the structural character and tectonic history of the Witwatersrand Basin. Precambr Res 177: 1–22

Davidson CF (1965) The mode and origin of banket orebodies. Institute of Mining and Metallurgy, London, Transcripts 74:319–338

de Wit MJ, Armstrong RA, Kamo SL, Erlank AJ (1993) Gold bearing sediments in the Pietersberg greenstone belt: age equivalents of the Witwatersrand Supergroup sediments. Econ Geol 88:1242–1252

Depiné M, Frimmel HE, Emsbo P, Koenig AE, Kern M (2013) Trace element distribution in uraninite from Mesoarchaean Witwatersrand conglomerates (South Africa) supports placer model and magmatogenic source. Miner Deposita 48:423–435

Drennan GR, Robb LJ (2006) The nature of hydrocarbons and related fluids in the Witwatersrand Basin, South Africa: Their role in metal redistribution. Geol Soc Am Spec Pap 405:353–385

Els BG (1998) The question of alluvial fans in the auriferous Archaean and Proterozoic successions of South Africa. S Afr J Geol 101:17–25

England GL, Rasmussen B, Krapez B, Groves DI (2002) Palaeoenvironmental significance of rounded pyrite in siliciclastic sequences of the Late Archaean Witwatersrand Basin: oxygen-deficient atmosphere or hydrothermal evolution. Sedimentology 49:1122–1156

Eriksson KA, Turner BR, Vos RG (1981) Evidence of tidal processes from the lower part of the Witwatersrand Supergroup, South Africa. Sed Geol 29:309–325

Farquhar J, Peters M, Johnston DT, Strauss H, Masterson A, Wiechert U, Kaufman AJ (2007) Isotopic evidence for Mesoarchaean anoxia and changing atmospheric sulphur chemistry. Nature 449:706–709

Feather C, Koen GM (1975) The mineralogy of the Witwatersrand reefs. Minerals Science and Engineering 7:189–224

Frimmel HE (1994) Metamorphism of Witwatersrand gold. Explor Min Geol 3:357–370

Frimmel HE (1997) Chlorite thermometry in the Witwatersrand basin: constraints on the Paleoproterozoic geotherm in the Kaapvaal Craton, South Africa. J Geol 105:601–615

Frimmel HE (2005) Archaean atmospheric evolution: evidence from the Witwatersrand gold fields, South Africa. Earth Sci Rev 70:1–46

Frimmel HE (2010) Verfügbarkeit von natürlich vorkommendem Uran. Unpublished Report, Office of Technology Assessment at the German Bundestag (TAB), Berlin, p 123

Frimmel HE (2014) A giant Mesoarchean crustal gold-enrichment episode: possible causes and consequences for exploration In: Kelley K, Golden HC (eds) Building exploration capability for the 21st Century. Society of Economic Geologists, Special Publication 18, pp 209–234

Frimmel HE (2018) Episodic concentration of gold to ore grade through Earth's history. Earth Sci Rev 180:148–158

Frimmel HE, Le Roex AP, Knight J, Minter WEL (1993) A case study of the postdepositional alteration of the Witwatersrand Basal reef gold placer. Econ Geol 88:249–265

Frimmel HE, Hallbauer DK, Gartz VH (1999) Gold mobilizing fluids in the Witwatersrand Basin: composition and possible sources. Mineral Petrol 66:55–81

Frimmel HE, Minter WEL (2002) Recent developments concerning the geological history and genesis of the Witwatersrand gold deposits, South Africa. In: Goldfarb RJ, Nielsen RL (eds) Integrated methods for discovery: global exploration in the twenty-first century. Society of Economic Geologists, Littleton, Special Publication 9, pp 17–45

Frimmel HE, Groves DI, Kirk J, Ruiz J, Chesley J, Minter WEL (2005) The formation and preservation of the Witwatersrand goldfields, the largest gold province in the world. In: Hedenquist JW, Thompson JFH, Goldfarb RJ, Richards JP (eds) Economic Geology One Hundredth Anniversary Volume. Society of Economic Geologists, Littleton, Colorado, pp 769–797

Frimmel HE, Zeh A, Lehrmann B, Hallbauer DK, Frank W (2009) Geochemical and geochronological constraints on the nature of the immediate basement beneath the Mesoarchaean auriferous Witwatersrand Basin, South Africa. J Petrol 50:2187–2220

Frimmel HE, Schedel S, Brätz H (2014) Uraninite chemistry as forensic tool for provenance analysis. Appl Geochem 48:104–121

Frimmel HE, Hennigh Q (2015) First whiffs of atmospheric oxygen triggered onset of crustal gold cycle. Miner Deposita 50:5–23

Fuchs S, Williams-Jones AE, Jackson SE, Przybylowicz WJ (2016) Metal distribution in pyrobitumen of the Carbon Leader Reef, Witwatersrand Supergroup, South Africa: Evidence for liquid hydrocarbon ore fluids. Chem Geol 426:45–59

Gartz VH, Frimmel HE (1999) Complex metasomatism of an Archean placer in the Witwatersrand basin, South Africa: The Ventersdorp Contact reef - a hydrothermal aquifer? Econ Geol 94:689–706

Gibson RL, Wallmach T (1995) Low pressure-high temperature metamorphism in the Vredefort Dome, South Africa—Anticlockwise pressure-temperature path followed by rapid decompression. Geol J 30:121–135

Gray GJ, Lawrence SR, Kenyon K, Cornford C (1998) Nature and origin of carbon in the Archean Witwatersrand Basin, South Africa. J Geol Soc, London 155:39–59

Gumsley A, Stamsnijder J, Larsson E, Söderlund U, Naeraa T, de Kock MO, Ernst R (2018) The 2789-2782 Ma Klipriviersberg large igneous province: implications for the chronostratigraphy of the Ventersdorp Supergroup and the timing of Witwatersrand gold deposition. Geocongress 2018, 18-20 July 2018, Johannesburg, Geological Society of South Africa, Abstract Book, p 133

Guy BM, Beukes NJ, Gutzmer J (2010) Paleoenvironmental controls on the texture and chemical composition of pyrite from non-conglomeratic sedimentary rocks of the Mesoarchean Witwatersrand Supergroup, South Africa. S Afr J Geol 113:195–228
Hallbauer DK, Joughin NC (1973) The size distribution and morphology of gold particles in the Witwatersrand reefs and their crushed products. J S Afr Inst Min Metall 1973:395–405
Hallbauer DK (1975) The plant origin of Witwatersrand carbon. Miner Sci Eng 7:111–131
Hallbauer DK (1986) The mineralogy and geochemistry of Witwatersrand pyrite, gold, uranium, and carbonaceous matter. In: Anhaeusser CR, Maske S (eds) Mineral deposits of Southern Africa. Geological Society of South Africa, Johannesburg, pp 731–752
Hayward CL, Reimold WU, Gibson RL, Robb LJ (2005) Gold mineralization within the Witwatersrand basin, South Africa: evidence for a modified placer origin, and the role of the Vredefort impact event. In: MacDonald I, Boyce AJ, Butler IB, Herrington RJ, Polya DA (eds) Mineral deposits and earth evolution. Geological Society, London, Special Publication 248, pp 31–58
Heinrich CA (2015) Witwatersrand gold deposits formed by volcanic rain, anoxic rivers and Archaean life. Nat Geosci 8:206–209
Henkel H, Reimold WU (1998) Integrated geophysical modelling of a giant, complex impact structure: anatomy of the Vredefort Structure, South Africa. Tectonophysics 287:1–20
Heubeck C (2019) The Moodies Group—a High-Resolution Archive of Archean Surface Processes and Basin-Forming Mechanisms. In: Kröner A, Hofmann A (eds) The Archaean Geology of the Kaapvaal Craton, Southern Africa. Springer, Heidelberg, Chap. 6, pp 203–239
Hölzing A, Frimmel HE, Voland V, Dremel K, Zabler S, Minter WEL (2015) The cover of Mineralium Deposita's anniversary volume uncovered. In: André-Mayer A-S, Cathelineau M, Muchez P, Pirard E, Sindern S (eds) Mineral resources in a sustainable world, Proceedings of 13th Biennial SGA Meeting, 24–27 August 2015. Université de Lorraine, Nancy, vol. 4, pp 1407–1410
Hofmann A, Bekker A, Rouxel O, Rumble D, Master S (2009) Multiple sulphur and iron isotope composition of detrital pyrite in Archaean sedimentary rocks: A new tool for provenance analysis. Earth Planet Sci Lett 286:436–445
Jolley SJ, Henderson HC, Barnicoat AC, Fox NPC (1999) Thrust-fracture network and hydrothermal gold mineralization: Witwatersrand Basin, South Africa. In: McCaffrey KJW, Lonergan L, Wilkinson JJ (eds) Fractures, Fluid Flow and Mineralization. Geological Society, London, Special Publication 155: 153–165
Kamo SL, Reimold WU, Krogh TE, Colliston WP (1996) A 2.023 Ga age for the Vredefort impact event and a first report of shock metamorphosed zircons in pseudotachylitic breccias and granophyre. Earth Planet Sci Lett 144:369–387
Kingsley CS (1987) Facies changes from fluvial conglomerate to braided sandstone of the early Proterozoic Eldorado Formation, Welkom Goldfieldd, South Africa. SEPM Spec Publ 39:359–370
Koglin N, Frimmel HE, Minter WEL, Brätz H (2010a) Trace-element characteristics of different pyrite types in Mesoarchaean to Palaeoproterozoic placer deposits. Miner Deposita 45:259–280
Koglin N, Zeh A, Frimmel HE, Gerdes A (2010b) New constraints on the auriferous Witwatersrand sediment provenance from combined detrital zircon U-Pb and Lu-Hf isotope data for the Eldorado Reef (Central Rand Group, South Africa). Precambr Res 183:817–824
Kositcin N, McNaughton NJ, Griffin BJ, Fletcher IR, Groves DI, Rasmussen B (2003) Textural and geochemical discrimination between xenotime of different origin in the Archaean Witwatersrand Basin, South Africa. Geochim Cosmochim Acta 67:709–731
Kositcin N, Krapez B (2004) SHRIMP U-Pb detrital zircon geochronology of the Late Archaean Witwatersrand Basin of South Africa: relation between zircon provenance age spectra and basin evolution. Precambr Res 129:141–168
Large RR, Meffre S, Burnett R, Guy B, Bull S, Gilbert S, Goemann K, Danyushevsky L (2013) Evidence for an intrabasinal source and multiple concentration processes in the formation of the Carbon Leader Reef, Witwatersrand Supergroup, South Africa. Econ Geol 108:1215–1241
Law JDM, Bailey AC, Cadle AB, Phillips GN, Stanistreet IG (1990) Reconstructive approach to the classification of Witwatersrand 'quartzites'. S Afr J Geol 93:83–92
Manzi MSD, Hein KAA, King N, Durrheim RJ (2013) Neoarchaean tectonic history of the Witwatersrand Basin and Ventersdorp Supergroup: new constraints from high-resolution 3D seismic reflection data. Tectonophysics 590:94–105
Marsh JS, Bowen MP, Rogers NW, Bowen TB (1989) Volcanic rocks of the Witwatersrand Triad, South Africa. II: Petrogenesis of mafic and felsic rocks of the Dominion Group. Precambr Res 44:39–65
Martin DM, Stanistreet IG, Camden-Smith PM (1989) The interaction between tectonics and mudflow deposits within the Main Conglomerate formation in the 2.8–2.7 Ga Witwatersrand Basin. Precambr Res 44:19–38
McCarthy TS (2006) The Witwatersrand Supergroup. In: Johnson MR, Anhaeusser CR, Thomas RJ (eds) The geology of South Africa. Geological Society of South Africa, Johannesburg, pp 155–186
Mellor ET (1917) The geology of the Witwatersrand. explanation to the geological map. Spec Publi Geol Survey S Afr 3:1–46
Minter WEL (1978) A sedimentological synthesis of placer gold, uranium and pyrite concentrations in Proterozoic Witwatersrand sediments. In: Miall AD (ed) Fluvial sedimentology. Canadian Society of Petroleum Geologists, pp 801–829
Minter WEL (1999) Irrefutable detrital origin of Witwatersrand gold and evidence of eolian signatures. Econ Geol 94:665–670
Minter WEL, Feather CE, Glathaar CW (1988) Sedimentological and mineralogical aspects of the newly discovered Witwatersrand placer deposit that reflect Proterozoic weathering, Welkom gold field, South Africa. Econ Geol 83:481–491
Minter WEL, Loen JS (1991) Palaeocurrent dispersal patterns of Witwatersrand gold placers. S Afr J Geol 94:70–85
Mossman DJ, Minter WEL, Dutkiewicz A, Hallbauer DK, George SC, Hennigh Q, Reimer TO, Horscroft FD (2008) The indigenous origin of Witwatersrand "carbon". Precambr Res 164:173–186
Nesbitt HW, Young GM (1982) Early Proterozoic climates and plate motions inferred from major element chemistry of lutites. Nature 299:715–717
Nwaila G, Frimmel HE, Minter WEL (2017) Provenance and geochemical variations in shales of the Mesoarchaean Witwatersrand Supergroup. J Geol 125:399–422
Phillips GN, Law JDM (1994) Metamorphism of the Witwatersrand gold fields: a review. Ore Geol Rev 9:1–31
Phillips GN, Law JDM (2000) Witwatersrand gold fields: geology, genesis and exploration. SEG Reviews 13:439–500
Phillips GN, Powell R (2011) Origin of Witwatersrand gold: a metamorphic devolatilisation-hydrothermal replacement model. Appl Earth Sci (Trans Inst Min Metall B) 120:112–129
Poujol M, Anhaeusser CR (2001) The Johannesburg Dome, South Africa: new single zircon U-Pb isotopic evidence for early Archaean granite-greenstone development within the central Kaapvaal Craton. Precambr Res 108:139–158
Poujol M, Kiefer R, Robb LJ, Annhaeusser CR, Armstrong RA (2005) New U-Pb data on zircons from the Amalia greenstone belt, Southern Africa: insights into the Neoarchaean evolution of the Kaapvaal Craton. S Afr J Geol 108:317–332
Ramdohr P (1958) New observations on the ores of the Witwatersrand in South Africa and their genetic significance. Trans Geol Soc South Africa 61:1–50

RMG (2015) Raw Materials Data Base. © Intierra Raw Materials Group, Stockholm
Robb LJ, Meyer FM (1991) A contribution to recent debate concerning epigenetic versus syngenetic mineralization processes in the Witwatersrand Basin. Econ Geol 86:396–401
Robb LJ, Davis D, Kamo SL, Meyer FM (1992) Ages of altered granites adjoining the Witwatersrand Basin with implications for the origin of gold and uranium. Nature 357:677–680
Robb LJ, Meyer FM (1995) The Witwatersrand Basin, South Africa: geological framework and mineralization processes. Ore Geol Rev 10:67–94
Robb LJ, Robb VM (1998) Gold in the Witwatersrand Basin. In: Wilson MGC, Anhaeusser CR (eds) The mineral resources of South Africa. Council for Geoscience, Pretoria, pp 294–349
SACS, South African Committee for Stratigraphy (1980) Part 1: Lithostratigraphy of the Republic of South Africa, South West Africa/Namibia and the Republics of Bophuthatswana, Transkei and Venda. Department of Mineral and Energy Affairs, Geological Survey, Pretoria
Schidlowski M (1981) Uraniferous constituents of the Witwatersrand conglomerates: ore-microscopic observations and implications for Witwatersrand metallogeny. US Geol Surv Prof Pap 1161: N1–N29
Smith AJB, Beukes NJ, Gutzmer J (2013) The composition and depositional environments of Mesoarchean iron formations of the West Rand Group of the Witwatersrand Supergroup, South Africa. Econ Geol 108:111–134
Spangenberg J, Frimmel HE (2001) Basin-internal derivation of hydrocarbons in the Witwatersrand Basin, South Africa: Evidence from bulk and molecular $\delta^{13}C$ data. Chem Geol 173:339–355
Sutton SJ, Ritger SD, Maynard JB (1990) Stratigraphic control of chemistry and mineralogy in metamorphosed Witwatersrand quartzites. J Geol 98:329–341
Therriault A, Grieve R, Reimold WU (1997) Original size of the Vredefort impact structure: implications for the geological evolution of the Witwatersrand Basin. Meteorit Planet Sci 32:71–77
Tinker J, de Wit M, Grotzinger J (2002) Seismic stratigraphic constraints on Neoarchean-Paleoproterozoic evolution of the western margin of the Kaapvaal Craton, South Africa. S Afr J Geol 105:107–134
Tucker RF, Viljoen RP, Viljoen MJ (2016) A review of the Witwatersrand Basin—The world's greatest goldfield. Episodes 39:105–133
Tweedie EB (1986) The Evander goldfield. In: Anhaeusser CR, Maske S (eds) Mineral deposits of Southern Africa. Geological Society of South Africa, Johannesburg, pp 705–730
Vennemann TW, Kesler SE, O'Neil JR (1992) Stable isotope compositions of quartz pebbles and their fluid inclusions as tracers of sediment provenance: Implications for gold- and uranium-bearing quartz pebble conglomerates. Geology 20:837–840
Vennemann TW, Kesler SE, Frederickson GC, Minter WEL, Heine RR (1995) Oxygen isotope sedimentology of gold- and uranium-bearing Witwatersrand and Huronian Supergroup quartz-pebble conglomerates. Econ Geol 91:322–342
Wallmach T, Meyer FM (1990) A petrogenetic grid for metamorphosed aluminous Witwatersrand shales. S Afr J Geol 93:93–102
Winter HdlR, Brink MC (1991) Chronostratigraphic subdivision of the Witwatersrand Basin based on Western Transvaal composite columns. S Afr J Geol 94:191–203
Young GM, von Brunn V, Gold DJC, Minter WEL (1998) Earth's oldest reported glaciation: physical and chemical evidence from the Archean Mozaan Group (−2.9 Ga) of South Africa. J Geol 106:523–538
Zeh A, Jaguin J, Poujol M, Boulvais P, Block S, Paquette J-L (2013) Juvenile crust formation in the northeastern Kaapvaal Craton at 2.97 Ga—Implications for Archean terrane accretion, and the source of the Pietersburg gold. Precambr Res 233:20–43